Energy & Environmental Science

ROYAL SOCIETY OF CHEMISTRY

PAPER

View Article Online
View Journal | View Issue

Check for updates

Cite this: *Energy Environ. Sci.*, 2023, **16**, 2518

Stepping away from purified solvents in reductive catalytic fractionation: a step forward towards a disruptive wood biorefinery process†

W. Arts, * K. Van Aelst, E. Cooreman, J. Van Aelst, S. Van den Bosch and B. F. Sels *

Lignin-first reductive catalytic fractionation (RCF) is an emerging lignocellulose biorefinery technology that produces a unique lignin-derived bio-oil rich in functionalized phenolics in addition to (hemi)cellulose products. We present here a novel industrial-scale process that achieves a drastic reduction of the costs and the CO_2 footprint of RCF biorefining through a reaction liquor and solvent recycle system by which the pristine solvent, here methanol, is enriched with reaction (by-)products resulting in novel solvent mixtures other than the pure solvent(s) (*e.g.*, methanol or methanol/water) commonly used in RCF. The impact of the liquor recycling %, a key process variable that determines the load on the crude oil distillation column for solvent recuperation, was systematically examined through a coupled techno-economic analysis (TEA) and life cycle assessment (LCA) of the RCF biorefinery processing 150 kton birch wood per year. These analyses showed that the lignin oil minimum selling price (MSP-RLO) and global warming potential (GWP-RLO) can be as low as 1000 € per ton and 1.5 $kgCO_2$ $kgProduct^{-1}$ at a high liquor recycling (>70%) as the fuel consumption and capital costs associated with energy provisioning are significantly reduced in this way. These modelling results were corroborated by lab-scale experiments that mimic the simulated unique solvent compositions. Solvent mixtures comprising methanol (40–65 vol%), methyl acetate (20–25 vol%), acetic acid (0–2 vol%), water (10–20 vol%), and crude lignin oil (10–20 vol%) enhance lignin extraction (90–95%), achieve high monomer yields (syringyl-monomer yield >20%) and stimulate hemicellulose co-extraction (>45%). In addition, novel lignin oil phenolics are produced by partial acetylation of propanol sidechains. The RCF biorefinery economics were improved by lowering the reaction time and temperature at high liquor recycling to limit the reactor capital costs. By halving the reaction time from 2 to 1 h, the MSP-RLO drops to ~800 € per ton despite a somewhat lower lignin oil productivity. Finally, the general applicability of this process design was shown by applying the integrated computational-experimental approach developed in this work on a softwood, and a hardwood with high moisture content.

Received 27th March 2023,
Accepted 14th April 2023

DOI: 10.1039/d3ee00965c

rsc.li/ees

Open Access Article. Published on 02 May 2023. Downloaded on 2/3/2026 7:13:05 AM.
This article is licensed under a Creative Commons Attribution 3.0 Unported Licence.

Broader context

In transitioning towards a sustainable chemical industry, lignocellulose biomass bears an enormous potential as a renewable carbon feedstock to manufacture chemicals and materials. Beside the lignocellulose carbohydrates, also the lignin, a hetero-aromatic biopolymer making up 15–30% of the plant biomass, must be effectively valorised into useful products, which remains challenging. Reductive catalytic fractionation (RCF) is a promising biorefinery step that fractionates lignocellulose into useful precursors for downstream applications namely, a carbohydrate pulp and bio-oil rich in lignin-derived phenolics. However, for RCF to be implemented and scaled to an industrial production process, the economic and environmental costs for solvent purification by distillation and the capital expenses associated with the large-volume reactors must be strongly diminished. This work presents a novel concept for an RCF biorefinery process where the use of an innovative recycling system leads to unique solvent compositions comprising the pristine solvent methanol, enriched with reaction (by-)products in RCF. In this way, the selling price and CO_2 footprint of the lignin oil product can be drastically reduced, making competition with fossil analogues possible.

Centre for Sustainable Catalysis and Engineering, Department of Microbial and Molecular Systems, KU Leuven, Celestijnenlaan 200F, 3001 Leuven, Belgium. E-mail: wouter.arts@kuleuven.be, bert.sels@kuleuven.be

† Electronic supplementary information (ESI) available: Detailed experimental procedures; supplementary figures and tables. See DOI: https://doi.org/10.1039/d3ee00965c

Introduction

For the chemical industry to deliver on the sustainability goals set by the Paris Climate Agreement, it will be pivotal to step

This journal is © The Royal Society of Chemistry 2023

Open Access Article. Published on 02 May 2023. Downloaded on 2/3/2026 7:13:05 AM. This article is licensed under a Creative Commons Attribution 3.0 Unported Licence.

away from fossil carbon feedstocks *viz.*, petroleum, gas and coal, and transition towards the use of renewable carbon resources for the production of sustainable chemicals.[1–3] Lignocellulose biomass is often seen as a suitable alternative in that regard.[4–7] It is an abundant carbon feedstock that grows almost anywhere on earth through a series of biosynthetic processes that capture atmospheric carbon and trap it as CO_2 into the chemical bonds of the complex (bio)polymers contained in the lignocellulose, namely cellulose, hemicellulose and lignin.[8–12] The valorisation of lignocellulose in traditional biorefining is aimed at producing a pure carbohydrate pulp, rich in (hemi-)cellulose, by removal of lignin, an heterogeneous aromatic polymer. In these biorefinery schemes, the lignin usually degrades and forms highly-condensed structures of low chemical reactivity that are often incinerated to produce low-grade energy.[13] This leaves a large potential of the lignocellulose in terms of quantity and quality – lignin is the largest source of naturally occurring aromatics on earth – unutilized.[14–16] Recently, multiple novel biorefinery concepts have attempted to overcome this typical drawback of traditional, carbohydrate-centred biorefining *e.g.*, by preventing lignin recondensation through either catalysis[17–22] or protection-group chemistry.[23–25] These technologies are generally referred to as lignin-first biorefining.[26,27]

One such a promising lignin-first biorefinery concept is reductive catalytic fractionation (RCF). In RCF, lignocellulose is fractionated into a carbohydrate pulp and lignin oil, rich in phenolic monomers and oligomers, at high temperature (200–250 °C) and pressure (50–100 bar) in an organic solvent, usually a short-chain alcohol (*e.g.* methanol), to which a redox catalyst (*e.g.*, Ru/C) and a hydrogen donor (*e.g.*, H_2) are added.[17,27,28] The irreversible recondensation of reactive lignin fragments, released from the lignocellulose matrix after simultaneous extraction and depolymerization of the native lignin, is prevented by a reductive stabilization step which is facilitated by the combined action of the redox-catalyst and hydrogen source.[29–31] RCF has known multiple conceptual alterations since its (re-)emergence in the past decade. The effect of the solvent composition,[19,32–37] catalyst formulation,[18,22,29,34,38–40] hydrogen donor,[19,20,35–37,41,42] and lignocellulose feedstock[17,18,21,31,43–45] on the delignification and lignin oil properties (*e.g.*, chemical functionality, monomer yield, molecular weight distribution *etc.*) in RCF have been extensively reported. Most of these studies were completed in a batch reactor mode, from small mL to larger L scale, which was later challenged by a flow-through system where the biomass and catalyst are physically separated in two independent fixed beds.[46–49] This reactor configuration allowed to study the kinetics of the main reaction steps *viz.*, solvolysis, reductive stabilization and recondensation independently, leading to a better understanding of the inherent relations between mass transfer and chemical reaction in RCF.[30,50]

The main products of the RCF biorefinery, the carbohydrate pulp and lignin oil are excellent precursors for multiple chemical products like fuels (*e.g.*, ethanol,[17] naphtha,[51] jet fuel[52,53]), platform chemicals (*e.g.*, phenol,[54,55] propylene,[55] ethylene glycol[56,57]), polymers (*e.g.*, polycarbonate,[58] polyurethanes,[52] epoxy resins[59,60]), coatings,[61] adhesives (*e.g.*, epoxy resin[62]), antioxidants,[63,64] surfactants,[25] *etc.* This signifies the large valorisation potential of lignocellulose biorefining with RCF.

For RCF to be feasible at industrial scale, it must fit within a larger processing framework in which chemical reaction and downstream separation processes are efficiently combined to convert lignocellulose into price-competitive and sustainable products.[65–67] Techno-economic analysis (TEA) and life cycle assessment (LCA) are well-known methodologies that enable to prematurely assess the economic and environmental performance of a novel chemical process by calculating typical performance indicators such as the minimum selling price (MSP) and the global warming potential (GWP) based on the technical framework provided by a detailed process simulation.[68] Such an assessment was first completed for RCF by Liao *et al.*[55] They presented an economically-competitive biorefinery producing a pulp, amenable to ethanol production and a lignin oil with RCF of birch lignocellulose. The lignin oil monomers were further processed into phenol and propylene with a series of catalytic steps, and the lignin oil oligomers were used in printing ink as replacement for *para*-nonylphenol, a controversial petrochemical.[55] LCA estimated that a lower CO_2 footprint (*i.e.*, −60%) could be achieved for these biorefinery products compared to their fossil-based counterparts.[55] This demonstrative study was followed by a more detailed analysis of Bartling *et al.*[50] They identified the major cost and environmental sustainability drivers of a similar RCF biorefinery process that produces a crude lignin oil and ethanol, obtained by enzymatic hydrolysis and fermentation of the pulp polysaccharides. The RCF area of their base case process consists of a reactor area, followed by a centrifugation step, to remove the solid pulp, and a two-stage distillation where the solvent, methanol, and water, released from the lignocellulose during RCF, are separated from the crude lignin oil in a first step, and the composition of the solvent recycle stream is tuned in the second step. The solvent methanol, which contains some water, is redirected to the reactor area and the remaining water is sent to a wastewater treatment unit. The major cost drivers identified with this process configuration were (i) the capital costs for the high-pressure reactors and (ii) the operational costs for the natural gas necessary to provide the process heat for the solvent distillation steps. It was suggested that priority should be given to RCF with a minimal solvent loading (*i.e.*, solvent-to-biomass ratio) to reduce capital expenses associated with large volume reactors and limit the energy requirements and corresponding fossil CO_2 emissions for solvent recuperation.[50] As a way to reduce the overall solvent usage, Jang *et al.* experimentally showed that lignin oil can be concentrated in the solvent – up to 12 wt% – without losing performance in terms of lignin removal and monomer yield in flow-through RCF.[48]

We present an innovative process configuration for an RCF biorefinery that produces a lignin oil, a carbohydrate pulp, and an aqueous stream rich in sugar-derivatives from birch

Open Access Article. Published on 02 May 2023. Downloaded on 2/3/2026 7:13:05 AM.
This article is licensed under a Creative Commons Attribution 3.0 Unported Licence.

lignocellulose at a drastically reduced cost and CO_2 footprint compared to previous reports. Supported by a more complete, experimentally verified mass balance for RCF with a pure solvent methanol and birch, we developed a new liquor and solvent recycle system with a reduced distillation load in which (i) methanol, (ii) methyl acetate and acetic acid, formed by hemicellulose deacetylation, and (iii) water, released from the lignocellulose matrix, are recycled back to the reactor area along with (iv) the crude lignin oil, containing lignin phenolics and methylated sugars. TEA and LCA of this RCF process configuration show that the capital expenses, the process heating costs, and CO_2 emissions can be significantly reduced at the steady-state composition of the solvent mixture that is obtained when the load on the crude oil distillation column is reduced by recycling part of the reaction liquor back to the reactor. Guided by the simulation results, we investigated and verified the technical feasibility and flexibility of this process configuration by experimentation with these solvent mixtures containing methanol, methyl acetate, water, acetic acid, and crude lignin oil in lab-scale RCF. Promisingly, a higher delignification, phenolic monomer yield and a purer pulp can be obtained with this multi-solvent system in which reaction (by-)products are partially enriched compared to pure methanol RCF. Presence of acetates in the solvent mixture also induced the formation of phenolics with acetylated C_3 sidechains, in this way, expanding the refinery's product portfolio. We also demonstrate that this process configuration can be further optimized for reaction time and temperature and is generally applicable to other feedstock types (*e.g.*, softwood). This study shows how an integrated approach combining process modelling and experimental research was exploited to innovate and optimize the RCF process towards an economically feasible and sustainable lignin-first biorefinery.

Results and discussion

RCF mass balance

The reactor mass balance of RCF, used as basis for the process simulation (see 'Process Description') (Fig. 1), was estimated from a detailed chemical analysis of a basic, lab-scale RCF reaction (100 mL reactor) with birch lignocellulose (4 g, extractive-free basis) in pure methanol (40 mL) using Pd/C as a solid redox catalyst (0.4 g) at typical reaction conditions of 220 °C and 30 bar H_2 at RT (~80 bar total pressure at 220 °C) which were maintained for 2 h. Purification of the reaction liquor by filtration and solvent evaporation resulted in a carbohydrate pulp and a crude lignin oil (CLO), which was further refined by liquid extraction with ethyl acetate and water to produce a refined lignin oil (RLO) and an aqueous sugar solution. Numerous techniques were used to analyse the mass consumption and formation in RCF (see Materials and methods and Section 1 of the ESI,† for a complete description of the methodology). Compositional analysis of the birch substrate and pulp product revealed that virtually all cellulose is retained, whilst some of the hemicellulose (12%) and a large amount of the lignin (63%) are removed from the lignocellulose. The acetyl-groups, attached to the xylan backbone of hemicellulose, are only partially retained in the pulp (retention of 20%). The refined lignin oil consists of phenolic monomers and oligomers

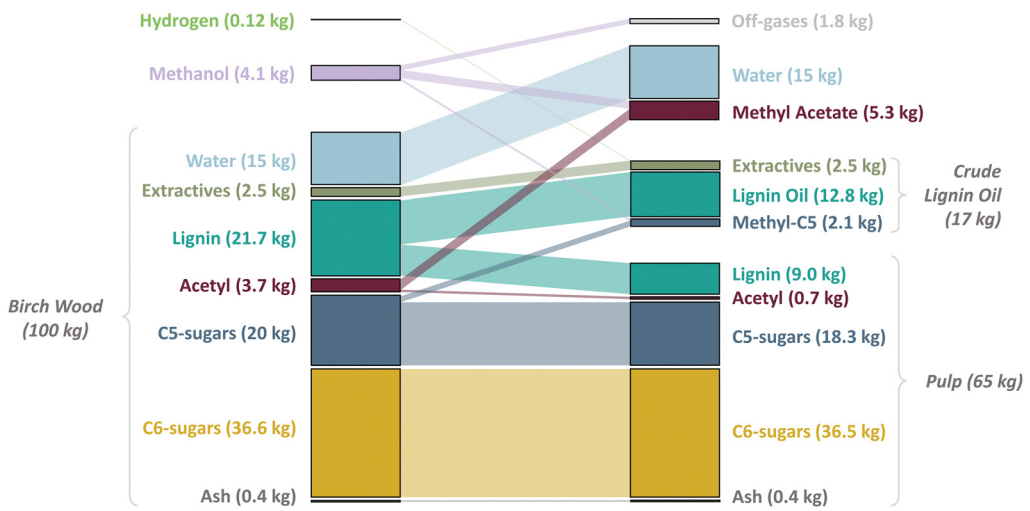

Fig. 1 Mass consumption and formation in RCF on a 100 kg birch wood basis. The lignocellulose was assumed to have a moisture content of 15 wt% on a wet basis to account for incomplete drying of wood chips used in industrial scale processes compared to wood sawdust (±5 wt%) used in lab-scale experiments. In line with our experimental analysis of the reaction liquor, it was assumed that all the water is released from the wood in RCF. The extractives, a diverse group of chemical compounds, though mainly apolar in nature, are only minorly present in the substrate with 2.5 wt%. They were assumed to behave similarly as the lignin oil components throughout the biorefinery process, hence end up in the crude lignin oil and eventually, in the refined lignin oil. Ash (0.4 wt%) was assumed to remain in the carbohydrate pulp. The consumption of methanol was estimated by the formation of methyl acetate and methylated sugars and its reformation to CO, CO_2 and other gaseous molecules analysed by off-gas analysis (Table S1, ESI†). Although the methylated C6 sugar derivatives were detected with GC-FID (Fig. S3, ESI†), they are not shown in this figure given their limited formation in RCF (<0.1 kg based on 100 kg of wood) as was determined by wood and pulp compositional analyses.

 This journal is © The Royal Society of Chemistry 2023

Open Access Article. Published on 02 May 2023. Downloaded on 2/3/2026 7:13:05 AM.
This article is licensed under a Creative Commons Attribution 3.0 Unported Licence.

and has a large selectivity to the 4-*n*-propanol substituted guaiacyl (11%) and syringyl (31%) monomeric units as shown by the lignin oil molecular weight distribution (Fig. S1, ESI†) and gas chromatogram (GC), respectively (Fig. S2, ESI†). The delignification degree (of 63%) and lignin oil composition signify a successful lignin extraction and depolymerization, and monomer stabilization, and are in line with our previous reports on hardwood – Pd/C RCF in methanol.[32,33,38] GC analysis of the aqueous solution indicated that the hemicellulose released from the lignocellulose is solvolytically depolymerized thereby consuming methanol. This is evidenced by the formation of multiple isomers of mainly methylated C5 and some methylated C6 sugar monomers (Fig. S3, ESI†). A detailed quantitative analysis of this stream is technically cumbersome; hence, we assumed a complete depolymerization of the extracted hemicellulose, in this way, assuming a worst-case scenario in terms of maximum methanol consumption. Methanol is also consumed by deacetylation of hemicellulose sugar units forming methyl acetate as was shown by GC analysis of the filtered reaction liquor (Fig. S4b, ESI†). This analysis along with the compositional analyses of the wood substrate and pulp enabled us to close the acetyl mass balance nearly to completion. Further, Karl-Fischer titration of the reaction liquor and moisture analysis of the substrate indicated that the water present in the pristine lignocellulose is fully released into the reaction liquor. Finally, the hydrogen consumption and methanol reforming were estimated from a post-reaction gas phase analysis (Table S1, ESI†). Using this extended experimental analysis, an unprecedented 98 wt% of the pristine wood substrate could be traced back in the RCF output flows. The reactor process mass balance was then scaled from the experimental mass balance following a few scale-up rules and assumptions (see caption of Fig. 1). For 100 kg of birch wood on a wet basis, 65 kg pulp, 17 kg crude lignin oil, 5.3 kg methyl acetate and 15 kg water are produced. 4.1 kg of methanol is consumed forming methyl acetate (5.3 kg) methylated sugars (2.1 kg) and off-gases (1.8 kg – CO, CO_2. *etc.*), by deacetylation and solvolytic depolymerization of (hemi-)cellulose and methanol reforming, respectively. Hydrogen consumption is limited to only 0.12 kg.

Process design

Process description. The reactor mass balance (Fig. 1) served as our starting point to build the innovative process configuration for the RCF biorefinery, which was simulated with the Aspen HYSYS® process simulation software. The biorefinery was designed to convert 150 kt wood per year (on a wet basis) into three product streams; (i) a refined lignin oil, (ii) a carbohydrate pulp, and (iii) an aqueous sugar stream. This scale is comparable to the capacity of a small-sized chemical pulping mill, and is expected to be sufficiently large to benefit from the economies of scale.[69] The biorefinery consists of three sections: (i) the reactor and liquor recycle area, (ii) the crude oil purification, and (iii) the combined heat and power plant (CHP). An overview of the process is given by the process flow diagram presented in Fig. 2.

The RCF reactor was modelled as a continuous system of 4 parallel reactors which convert wood into pulp, crude lignin oil, methyl acetate and water, according to an extrapolated reactor mass balance shown in Fig. 1 for 100 kg of wood. The methyl acetate hydrolysis/esterification equilibrium reaction was also modelled based on the molar amounts of methyl acetate, water and methanol to account for methyl acetate hydrolysis to acetic acid. We assumed chemical equilibrium of this reaction with an equilibrium constant of 0.06 for the forward hydrolysis and backwards esterification reaction at elevated temperatures (>200 °C).[70] It was also assumed that the catalyst is physically separated from the biomass to avoid a difficult solid–solid separation which can be achieved in practice by a flow-through

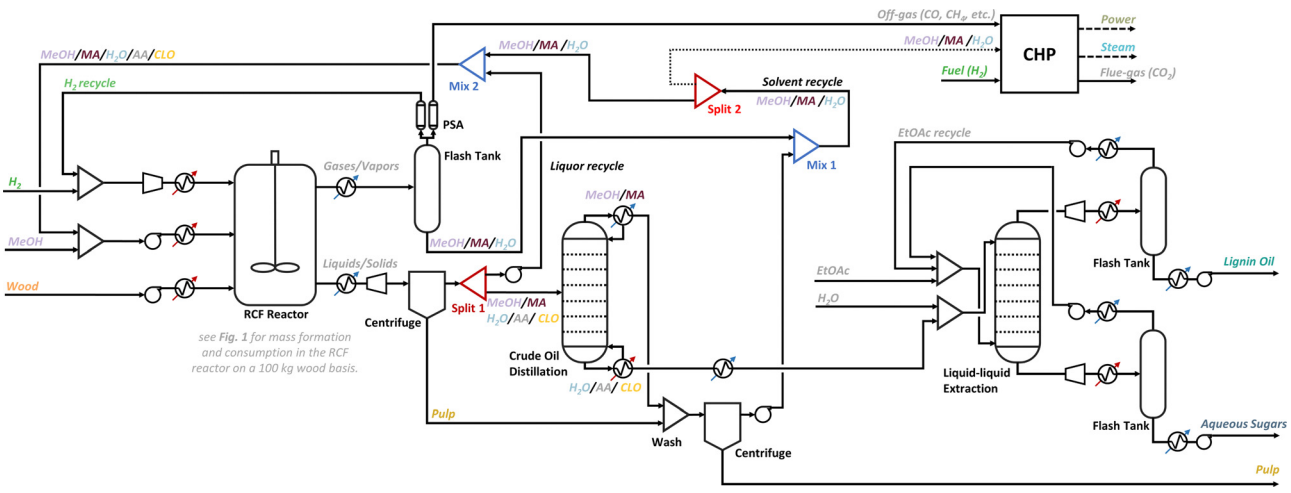

Fig. 2 Process flow diagram of the RCF biorefinery. The biorefinery consists of three sections: (i) the reactor and recycle area, where wood is converted, the reaction mixture is purified and solvents are recycled; (ii) the crude oil purification which produces a refined lignin oil an aqueous sugar solution by liquid–liquid extraction and (iii) the combined heat and power plant (CHP), which produces the power and heat that is consumed by the process by recuperating the chemical energy contained in the off-gases and process purge streams. Abbreviations: MeOH – methanol, MA – methyl acetate, AA – acetic acid, CLO – crude lignin oil, EtOAc – ethyl acetate.

Open Access Article. Published on 02 May 2023. Downloaded on 2/3/2026 7:13:05 AM. This article is licensed under a Creative Commons Attribution 3.0 Unported Licence.

system[30,47–49] or batch system with catalyst basket.[29,65] Despite that a fully continuous reactor does not yet exist for RCF, it allows to study the integration of the reactor mass in- and outflows with the downstream processing, which is the main purpose of this work. Even with a system of parallel batch or flow-through reactors acting as a continuous system, a similar integration of the reactor mass flows within the entire process, as proposed here, can be achieved. Solvent is added to the reactor at a ratio of 10 L (at RT) per kg of dry biomass which is comparable to the lab-scale solvent-to-biomass ratio (see 'RCF mass balance'). The solvent stream must be supplemented with fresh methanol to account for solvent losses in the reaction and downstream processing and to ensure a constant volumetric flow rate (at RT). Similarly, hydrogen is fed to the reactor at a rate of 0.05 kg hydrogen per kg of dry biomass (± conform the loading of hydrogen in the lab reactor at 30 bar at RT), and make-up hydrogen is added to a gas recycle stream to account for hydrogen consumption in RCF. The reactor inlet streams *viz.*, the fresh wood, solvents and hydrogen are conditioned to 220 °C and 90 bar before reactor entry. After RCF, which lasts 2 h, the gases and vapours are removed from the reactor *via* an in-line flash at high temperature and pressure and are subsequently cooled and fed to a flash tank to separate the gases from the vapours *viz.*, methanol, methyl acetate and some water, which are recovered as a liquid. Excess hydrogen is purified from the gaseous stream containing some short-chain alkanes, CO and CO_2 by pressure swing adsorption (PSA), which was modelled as a component split, and is recycled to the reactor section. The reaction slurry is cooled down to suppress chemical reaction, depressurized, and filtered by centrifugation. The resulting liquid stream contains methanol, methyl acetate, water, crude lignin oil and some acetic acid and is fed to the crude oil distillation column. This column was designed to recover 99.9% of the inlet methanol (the light key component) in the overheads stream, with minimal entrainment of water (the heavy key component). Methyl acetate, having a lower boiling-point than methanol at the column operational pressure (2 bar), is always recuperated in the overhead stream as well. The bottoms stream of the column consists of water, the crude lignin oil, some acetic acid, and contains only little methanol. Methanol and methyl acetate of the overheads are used in a pulp washing step before being mixed with the flash tank condensate (mix 1), whilst the bottoms stream is fed to the crude oil purification section. Prior to the crude oil distillation, the liquid stream can be split at a predefined ratio (split 1) into two streams. Only one stream is fed to the column whilst the other, *i.e.*, the liquor recycle, is pressurized and mixed (mix 2) with the condensate recycle stream of the flash tank and the distillation overheads stream. The resulting liquid stream contains methanol, methyl acetate, acetic acid, water, crude lignin oil and is redirected to the reactor section where fresh methanol is added to maintain the set volumetric flow rate of 10 L solvent (at RT) per kg dry wood. The liquid stream obtained in mix 1 can be purged (dotted line – split 2) prior to mixing in mix 2, to control the solvent composition, and in particular, the enrichment of methyl acetate in the solvent recycle stream.

The crude lignin oil is further purified by liquid–liquid extraction with ethyl acetate and water resulting in an organic phase, enriched with the lignin oil phenolics, and an aqueous phase, containing the methylated sugar derivatives. The amount of water and ethyl acetate used in the liquid–liquid extraction was set to 1.1 kg of each, per kg of crude lignin oil to ensure a good separation. Most of the water necessary for the extraction is already present in the bottoms stream of the distillation and only a small amount of fresh ethyl acetate needs to be added as most is recycled from the organic phase by a vacuum flash operation (at 0.5 bar), producing the refined lignin oil and the ethyl acetate recycle stream. Ethyl acetate is also recuperated from the aqueous stream containing the methylated sugars by a similar vacuum flash operation at low temperature (50 °C) to avoid sugar degradation. Water is not recuperated and leaves the biorefinery with the methylated sugars along with acetic acid that has concentrated up to 10 wt% in this stream. Recovery of acetic acid from this stream can be considered but was not investigated here.

The CHP providing power and heating to the biorefinery is supplied with off-gases and purge streams (if any) from the refinery. A schematic overview of the CHP is depicted in Fig. S5 (ESI†). The off gases are combusted at high temperature and pressure in the gas turbine generating power upon expansion of the combustion gases to low pressure. The heat of the flue gas is recuperated by the production of steam in a steam boiler. Additional fuel can be supplied, in case of large heating requirements. We opted for hydrogen as the ultimate energy vector as it is already provided on site for chemical reaction and it bears a significant potential as a renewable energy vector to fuel chemical production processes in the future.[71]

Operation of the liquor recycle system. One major variable in the operation of the liquor recycle system, and thereby the entire process, is the ratio by which the filtered reaction liquor is split between the recycle stream and the crude oil distillation (Fig. 2, split 1). This ratio is hereafter referred to as the liquor recycling (expressed in %). The main goal of this liquor recycle is to decrease the load on the crude oil distillation column. We anticipated that, along with the recycling of methanol and methyl acetate after distillation, the energy requirements of the biorefinery can be drastically cut in this way, by reducing the distillation volumes of the solvents as compared to the two-step distillation process presented by Bartling *et al.*, where the entire reaction liquor is purified before re-entry of the solvent in the reactor.[50] However, the liquor recycle affects the mass flow and composition of multiple process streams, including the inlet solvent stream of the reactor. Its impact on the process operation was therefore investigated using the steady-state process simulation. In this initial assessment, it was assumed that the formation of products from the birch wood and the consumption of methanol and hydrogen (Fig. 1) do not change with increasing liquor recycling rates, although this is likely not the case. This important assumption, which allowed us to explore the recycling system in the first place, is verified, as

 This journal is © The Royal Society of Chemistry 2023

Open Access Article. Published on 02 May 2023. Downloaded on 2/3/2026 7:13:05 AM.
This article is licensed under a Creative Commons Attribution 3.0 Unported Licence.

discussed in the experimental section of this work (see 'Model-driven experimental RCF'). The purge ratio (0.01%, split 2) and the distillation column design specifications were kept constant throughout the simulations. The dynamics of the recycle system are not studied here in depth. Nonetheless, the recycle loops take on average 15 iterations to reach a feasible steady state. As indication, this would correspond to 30 hours of operation or 0.3% of the total operation time.

When all liquid is distilled, *i.e.*, at zero liquor recycling, the methanol solvent stream is primarily enriched with methyl acetate (26 vol%) along with some water (1 vol%) originating from the flash tank liquid (Fig. 3). The concentration of the crude lignin oil and water increase at higher liquor recycling, though only minorly due to the relatively high solvent-to-biomass ratio of 10 L kg^{-1} and a low wood conversion of 35% (Fig. 1). For example, the solvent contains 7 vol% water and 6 vol% crude lignin oil at a liquor recycling of 70%. Only at the highest recycling rates (*i.e.*, 90%), the inlet solvent stream becomes highly concentrated with water (18 vol%) and crude lignin oil (21 vol%), making up 39% of the solvent volume. Acetic acid is only minorly concentrated in the inlet solvent stream (<3 vol%), as its formation in the reactor is limited (especially at low liquor recycling) and because it is removed *via* the crude oil distillation bottoms stream given its higher boiling point than water, thereby escaping the solvent recycle stream. The composition of the liquid entering the crude oil distillation column shows a similar trend as the inlet solvent stream (Fig. S6, ESI†). More crude lignin oil and water become concentrated in this stream which also simplifies the solvent recuperation. The liquor recycling rate also affects the volumetric flow rate of the solvent at the fixed reactor conditions of 220 °C and 90 bar. The flow rate decreases with an increasing liquor recycling as less volatile water and crude lignin oil become more concentrated in the solvent, resulting in a smaller volumetric expansion at reaction temperature (−20% and −25% at 70% and 90% liquor recycling, respectively, compared to 0%). This implies that the reactor can be smaller, especially at high liquor recycling, which is an added advantage on top of reduced energy demand at reduced distillation loads. At 95% liquor recycling and above, the operation of the liquor recycle system was found to be infeasible as the design criterion *i.e.*, the solvent-to-biomass ratio of 10 L kg^{-1} at RT for the inlet solvent stream is violated. At these high liquor recycling rates, the additional liquid mass formed in RCF, from which most is recycled, causes the solvent-to-biomass ratio at RT to surpass 10 L kg^{-1}, making the make-up methanol redundant. The solvent composition then converges to a mixture of water, acetic acid, and crude lignin oil. Contra-intuitively, the total reactor volume required to accommodate RCF at reaction conditions is lower as the denser solvent mixtures are less volatile at high liquor recycling. It must also be noted here that in an industrial scale process, reactor volumes are fixed and cannot 'change'. However, steady state conditions can be reached with smaller, but fixed reactor volumes, by decreasing the reactor temperature (reducing liquid expansion) and/or time (reducing required processing volumes) during start-up

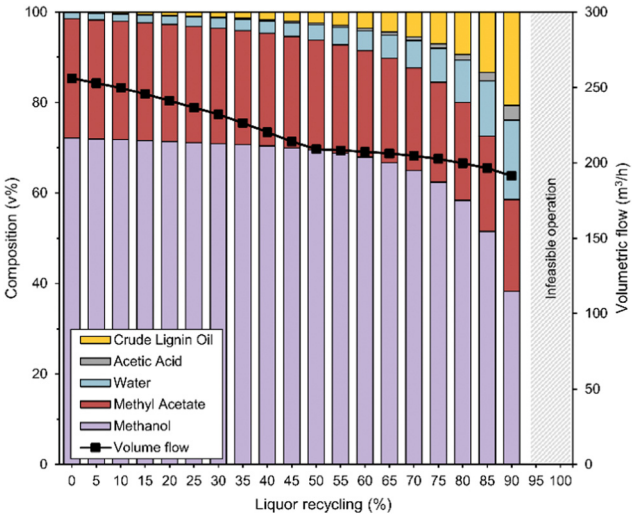

Fig. 3 The solvent composition at the reactor inlet (left axis) and solvent inlet volumetric flow rate at reaction conditions (right axis) in function of the liquor recycling (%) (*x*-axis). The liquor recycling represents the percentual amount of the filtered liquid reaction mixture that is recycled back to the reactor inlet as parameterized in split 1 (see Fig. 2). The solvent volumetric flow rate at reaction conditions depends on the overall solvent composition at the reactor inlet. Fresh methanol is added to the recycled streams to maintain a constant volumetric flow of 10 L per kg dry biomass at RT. At a liquor recycling of 95% and above, the operation of the liquor recycle was found to be infeasible as this design criterion is violated (see 'Operation of liquor recycle system').

of the operation, and/or by employing similar, less volatile solvent mixtures as predicted by the steady-state simulation from the beginning of the refinery operation and/or by recycling all reaction liquor without any purification in the start-up phase.

The altering mass and energy balances of the RCF biorefinery at a liquor recycling of 0, 50, 70 and 90% show that the process requires less energy at a reduced load on the crude oil distillation column (Table 1). The intake of fuel (*i.e.*, hydrogen) to produce steam decreases by 74%, from 2305 kg h^{-1} to 607 kg h^{-1}, at a high liquor recycling of 70% compared to 0%. The electric power, mainly required for the cooling water pump around, shows a similar trend. Its consumption decreases by 78% (from 2107 kW to 464 kW) for a liquor recycling of 70% compared to 0%. A 3-fold decrease in water consumption between these liquor recycling rates is also illustrative for the reduced cooling demands. When 90% of the reaction liquor is recycled, much less fuel, power and cooling water is needed. The fuel consumption drops to 13 kg hydrogen h^{-1}, excess electric power is generated (−251 kW) and cooling water input decreases almost 9-fold. However, the flue gas CO_2 emissions increase to 973 kg h^{-1} as more methanol and methyl acetate leave the reactor and recycle area *via* off-gas streams which are combusted in the CHP. Part of the energy is thus provided by wood acetyls and methanol. The need for less energy at high liquor recycling is also exemplified by the ratio of the energy content of fuel and the wood heating value. The energy input without liquor recycling is equivalent to 97% of

Open Access Article. Published on 02 May 2023. Downloaded on 2/3/2026 7:13:05 AM. This article is licensed under a Creative Commons Attribution 3.0 Unported Licence.

Table 1 Mass & energy balances of the RCF biorefinery at a liquor recycling of 0%, 50%, 70% and 90%. Aspen energy Analyzer® tool was used to optimize the heat exchanger network of the process (excluding the CHP) simulated in Aspen HYSYS®. A net heat, cooling and power loading of the process were estimated and used in CHP calculations for the steam and electricity production. Water is consumed in the liquid–liquid extraction, in the cooling water network and in the boilers for steam production. The catalyst used in the RCF biorefinery at a 1 : 10 catalyst/biomass ratio was assumed to have a lifetime of 2 year. The ratio of the biorefinery energy input and the wood calorific value was approximated by division of the heating value of methanol and fuel input and the power input by the heating value of the wood

		Liquor recycling (%)			
		0%	50%	70%	90%
Mass streams in/out (kg h^{-1})					
Input	Wood feedstock	17 473	17 473	17 473	17 473
	Methanol	631	342	448	403
	Hydrogen (RCF)	21	21	21	21
	Catalyst	0.1	0.1	0.1	0.1
	Ethyl acetate	63	81	80	86
	Water	124 224	68 505	43 600	15 997
Output	Lignin oil	2879	2871	2870	2875
	Pulp	11 327	11 327	11 327	11 327
	Aqueous sugars	278	287	297	287
Waste	Flue gas CO_2	585	608	647	973
Energy streams in/out					
	Fuel (H_2) (kg h^{-1})	2305	1126	607	13
	Electric power (kW)	2107	979	464	−251
Energy input/LHV wood (%)		97%	47%	26%	0.5%

the wood heating value. This ratio decreases to 47, 26 and 0.5% at a liquor recycling of 50, 70 and 90%, respectively. Our one step distillation process with a reduced load on the distillation column at high liquor recycling performs thereby significantly better than the two-step distillation process reported earlier in which the recycling of reaction by-products and crude lignin oil was not considered. Here, the process heating for distillation alone equalled 73% of the wood heating value already.[50] Note that very little hydrogen (21 kg h^{-1}) is consumed in the RCF reaction which is much less compared to the fuel requirements of the refinery, especially at low liquor recycling (see Hydrogen (RCF) *vs.* Fuel (H_2) in Table 1).

Process economics and CO_2 footprint

To investigate if and to what extent this novel design could have affected the economics and environmental impact of the RCF biorefinery, we conducted a techno-economic analysis (TEA) and life cycle assessment (LCA) of the process by which typical performance metrics such as the minimum selling price (MSP-RLO) and the global warming potential (GWP-RLO) of the refined lignin oil, respectively, were calculated. We chose to estimate these metrics for the lignin oil in particular, as no such product is currently marketed compared to the carbohydrate pulp which can be regarded as an established product and represents ~98% of the other product revenues. The mass and energy balances obtained with the process simulation (Table 1) were used for estimating the operational expenses (OPEX). Capital expenses (CAPEX) were calculated using the factorial cost estimation method for which equipment sizing data was directly obtained or estimated from the Aspen HYSYS® process simulation (see 'Materials and methods'). The process economics, including the CAPEX, were re-evaluated at increasing liquor recycling rates given its impact on the process, as illustrated by the altering mass and energy balances of the refinery.

Operational and capital expenditure. The operational and the capital costs both decrease with a reducing load on the distillation column. Following the reduced process heating and cooling requirements for crude lignin oil distillation at high liquor recycling (Table 1), the operational costs to refine 150 kt wood per year decrease from 67 to 40 M€ per year, *i.e.*, a 40% reduction, between 0 and 90% liquor recycling (Fig. 4A). This is illustrated by the decreasing purchase costs for fuel (21–0.1 M€ per year) and electricity (1.8 to −0.2 M€ per year) which combined, give a significant cost decline of 23 M€ per year between a 0 and 90% liquor recycling, respectively. With an annual cost of 24.2 M€, the largest contribution to the operational expenses (34–57%) comes from the purchased wood feedstock, which remains constant at varying liquor recycling. Despite its high price (2100 € per t), the ethyl acetate purchase costs contribute only between 2 to 5% of the total operational expenditure as it is extensively recycled from the organic and aqueous streams leaving the liquid–liquid extractor. The capital costs are affected by the liquor recycling in two ways (Fig. 4B). First, as the distillation tower and CHP plant need to process less mass and provide less energy at high liquor recycling, they can be scaled down resulting in lower capital costs. The heat exchanger network (HEN) follows this trend in terms of the required heat exchangeable area. Capital expenditures for the distillation column, CHP and HEN decrease from 9.7 to 0.8 M€, 21.3 to 3.4 M€, and 25 to 12 M€, respectively, between a liquor recycling of 0 and 90%. Second, the smaller volumetric expansion of the solvent at high liquor recycling implies that the reactor volume can be reduced whilst maintaining a consistent operation at constant reaction conditions of 220 °C and 90 bar (see 'Process description'). The volume for each of the four reactors declines from 391 to 289 m^3 between a liquor recycling of 0 and 90%, respectively. Accordingly, the reactor costs decrease from 98 to 77 M€. With a share between 60 and 75%, the reactor costs contribute the most to the total capital expenditure which decreases from 163 to 103 M€ (−37%).

Minimum selling price of the lignin oil. One of the major cost drivers of the RCF biorefinery as identified by Bartling *et al. viz.*, the fuel costs for distillation, is tackled with this process configuration in which the solid-free reaction liquor is extensively recycled before distillation as shown by the OPEX (Fig. 4A). Another significant cost driver identified in their work *viz.*, the capital costs for high-pressure reactors, is reduced as well but together with and in a similar order of magnitude as the equipment costs for distillation, heat exchanging and the CHP (Fig. 4B). The reduced operational and capital expenses result in a significantly lowered MSP-RLO (Fig. 5A). We marked the selling price of benzene, phenol,

 This journal is © The Royal Society of Chemistry 2023

Open Access Article. Published on 02 May 2023. Downloaded on 2/3/2026 7:13:05 AM.
This article is licensed under a Creative Commons Attribution 3.0 Unported Licence.

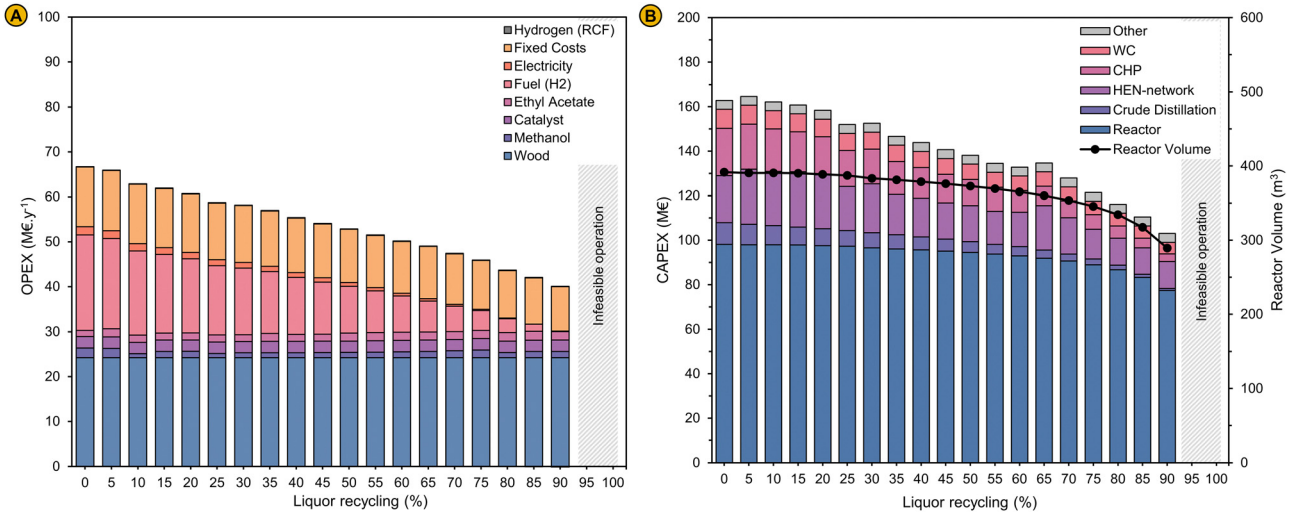

Fig. 4 (A) Operational expenditures (OPEX) in million € per year (M€ per year) and (B) capital expenditures (CAPEX) in million € (M€) of an RCF biorefinery processing 150 kt wood per year in function of the liquor recycling. A description of the cost estimation methods is given in the Methods and materials sections. The parameters for the cost calculations of the OPEX and CAPEX are presented in Tables S5 and S6 of the ESI.†

and bisphenol A (BPA) in Fig. 5A to position the lignin oil within the market of aromatic and phenolic petrochemicals, where it could become competitive as a bio-based alternative in the long term. We also depicted the (minimum) selling price of lignin oil, as estimated for previously reported process designs, as indication, but we do not want to draw any conclusions from this as these alternative designs serve other objectives and use different parameter values in their economic evaluation. For comparison of the MSP-RLO with other chemicals and fuels, we refer the reader to the TEA conducted by Bartling *et al.* and a review of Lynd *et al.* where detailed pricing and global production volumes of multiple chemical compounds are given.[50,72]

When the process is operated without liquor recycling, the MSP-RLO (2261 € per t) is larger than estimated before. This can be attributed to the high costs for the fuel hydrogen and the large capital expenses. At a liquor recycling rate of ~50%, the MSP-RLO coincides with the BPA selling price (1500 € per t) but still exceeds the selling price of phenol (1100 € per t) and benzene (400 € per t). For this price to be competitive, the added value of the lignin oil mixture should be comparable to pure BPA. This seems rather unlikely as until now, the lignin oil needs additional processing to yield monomer derived bisphenols[73] or oligomers that are equivalent to BPA[62] and there is no margin for this at a BPA selling price. Nevertheless, at high liquor recycling of >75%, the MSP-RLO decreases to below 1000 € per t, in between the phenol and benzene selling prices. This MSP agrees better with its role as a platform for phenolics as it allows for additional downstream processing and upgrading to chemicals equivalent to phenol, BPA and others, which have higher prices. This analysis signifies that the refinery design can become economically feasible if a high liquor recycling can be technically achieved.

Global warming potential of the lignin oil. In parallel with our economic assessment, we analysed the environmental impact of the RCF biorefinery at varying liquor recycling. We selected the GWP as the main environmental assessment criterion to evaluate the potential impact of the biorefinery on climate change. The GWP of the production of 1 kg of refined lignin oil (GWP-RLO) was estimated over a period of 100 years for a cradle-to-gate system with the RCF biorefinery being the final step in the value chain as shown in Fig. S7 (ESI†). Unlike with the LCAs conducted by Liao *et al.*[55] and Bartling *et al.*,[50] and inspired by recent work of Navare *et al.*,[74] we did not adopt the carbon neutrality principle in developing our LCA. This principle presumes that the uptake and emission of biogenic carbon, *i.e.*, the carbon originally embedded in the plant biomass, are equally balanced. However, the contribution of biogenic carbon emissions to the GWP depends on the rate of carbon sequestration and emission and the latter is not always known for the outputs of a cradle-to-gate system. The negative CO_2 emissions that are usually assigned to the wood feedstock to account for carbon sequestration by photosynthesis are therefore not always justified, for example, if the lifetime of the carbon embedded in the products is not sufficiently long with respect to the biomass rotation time. Moreover, this negative credit may overshadow the CO_2 emissions generated by the processes of the value chain (*i.e.*, the process CO_2 emissions) which complicates to study the impact of RCF process parameters on the LCA. Guest *et al.* introduced a CO_2 accounting system that elegantly resolves this matter.[75] They multiply the biogenic carbon emissions by an appropriate characterization factor (CF) whose value depends on the biomass rotation time and the life time of the biogenic carbon to correct for the relative rate of carbon uptake and emission. Following their method, we excluded the negative CO_2 emissions associated with carbon sequestration and used an appropriate CF of 0.2 to properly account for the biogenic CO_2 emissions generated by the process which have a zero lifetime (see 'Material and methods'). We maintained the cradle-to-gate system boundary to avoid estimating the lifetime of the carbon

Open Access Article. Published on 02 May 2023. Downloaded on 2/3/2026 7:13:05 AM.
This article is licensed under a Creative Commons Attribution 3.0 Unported Licence.

embedded in the refinery products. The resulting GWP thus corresponds to all process CO_2 emissions related to the production of 1 kg of RLO, which allows for a better comparison with the CO_2 footprints of fossil-based chemicals such as benzene, phenol, and BPA (Fig. 5B). The GWP values shown here are estimated when non-renewable energy vectors *viz.*, grey hydrogen and an electricity mix are used in the RCF biorefinery, but anticipating a widespread decarbonization of energy production, we also provide GWP values when using renewable energy vectors *viz.*, green hydrogen and wind electricity (Fig. S8 and S9, ESI†).

We calculated the GWP-RLO at varying liquor recycling rates by leveraging the process mass and energy balances (Table 1) to the life cycle inventory of the LCA. The GWP decreases from 4.42 to 0.71 $kgCO_2\ kgRLO^{-1}$ between a liquor recycling of 0 and 90%, which is consistent with the reduced energy requirements at a lower distillation load (Fig. 5B). This is exemplified by a decreasing footprint of the hydrogen fuel input (3.60–0.02 $kgCO_2\ kgRLO^{-1}$). The CO_2 footprint of the wood feedstock remains constant (0.45 $kgCO_2\ kgRLO^{-1}$), but is positive, as it solely represents the CO_2 emissions associated with harvesting and processing of birch trees to wood chips. At low liquor recycling the GWP-RLO exceeds the GWP of BPA (3.49 $kgCO_2\ kg^{-1}$), but at a liquor recycling above 65%, it drops to below the GWP of phenol (2.79 $kgCO_2\ kg^{-1}$) and benzene (1.86 $kgCO_2\ kg^{-1}$). Here, the margin is expected to be large enough for the GWP of lignin oil derived products to increase in downstream production processes but to remain below the GWP of fossil analogues *viz.*, phenol and BPA. The GWP-RLO is lower than the GWP of BPA, phenol, and benzene in all instances when renewable energy vectors are used (Fig. S9, ESI†). When including CO_2 capture through photosynthesis under the carbon neutrality principle the GWP-RLO decreases by 4.9 $kgCO_2\ kgRLO^{-1}$ in all instances, w/ and w/o renewable energy vectors (see Fig. S10, ESI† for the LCA system boundaries). As anticipated, the process CO_2 emissions contribute considerably less, relatively to the total GWP under the carbon neutrality principle, even when using non-renewable energy vectors. Given the significance of the applied methodology on the LCA results, we intend to provide detailed life cycle calculations elaborating on the carbon neutrality principle and its impact on the LCA for all process in- and outputs, in a follow-up communication. The purpose of the work presented in this section, is to show how LCA can be usefully applied to innovate and optimize the process.

Model-driven experimental RCF

The techno-economic assessment and environmental impact analysis demonstrate that the lignin oil can be produced at an economically viable selling price and with a low CO_2 footprint as shown by its MSP and GWP, respectively. However, for these performance metrics to be reliable, it is pivotal that the implementation of the corresponding simulation case is technically feasible. The key variable of the process is the liquor recycling as it directly determines the RCF solvent composition and volumetric flow rate at reaction conditions (Fig. 3). The

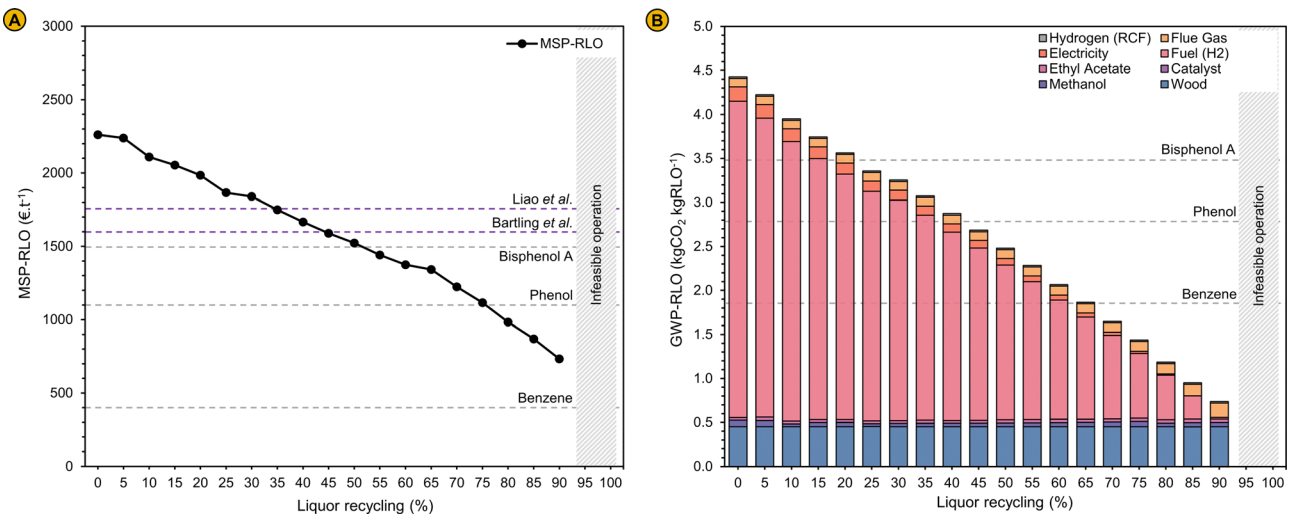

Fig. 5 (A) Minimum selling price of the refined lignin oil (MSP-RLO) in € per t in function of the liquor recycling. The selling price of benzene, phenol and bisphenol A were obtained from ICIS reports for the period 2019–2020.[88–90] In the work of Liao *et al.*, the selling price of the lignin oil oligomers was set to 1750 € per t to ensure an economic feasible operation of the biorefinery that also converts the lignin monomers to phenol for which a selling price of 1300 € per t was used.[55] The MSP-RLO estimated by Bartling *et al.* amounts 1600 € per t for their base design with methanol RCF. In their design, the pulp is fermented to bio-ethanol that is sold for 500 € per t.[50] The selling price of the pulp in this work was set to 400 € per t carbohydrates in the pulp similar to Liao *et al.*[55] (B) Share of the process in- and outputs to the global warming potential of the refined lignin oil (GWP-RLO) when an electricity mix and grey hydrogen (fuel) are used as energy vectors in function of the liquor recycling, compared to the GWP of benzene, phenol and bisphenol A. These GWP values correspond to the process CO_2 emissions solely and do not include negative emissions originating from biogenic carbon uptake by plant photosynthesis. GWP-RLO values when renewable electricity and green hydrogen are used as the refinery energy vectors are shown in Fig. S9 (ESI†). A description of LCA methdology is given in the Methods and materials section. The GWP parameters for the refinery in- and outputs are shown in Table S7 of the ESI.†

 This journal is © The Royal Society of Chemistry 2023

Open Access Article. Published on 02 May 2023. Downloaded on 2/3/2026 7:13:05 AM.
This article is licensed under a Creative Commons Attribution 3.0 Unported Licence.

effect of this variable was studied by assuming a constant formation of products from the birch wood and a fixed consumption of methanol and hydrogen according to the standard methanol reaction (see 'Operation of the liquor recycle system') as it could not be predicted beforehand how the RCF reaction would be affected by the new solvent compositions at varying liquor recycling given the multitude of variables to consider. Therefore, to assess whether the implementation of this design bears any potential in the first place, we compared RCF using the solvent mixtures as predicted by these preliminary simulations at varying liquor recycling with pure methanol RCF in a laboratory setting. Typical experimental performance indicators such as the pulp delignification, the lignin oil monomer content and molecular weight, and others were analysed to examine how the RCF reaction, and the quality of the refinery products are affected by liquor recycling (see 'Impact of liquor recycling'). The experimental results were then re-inserted in the simulation to analyse the impact of liquor recycling on the technical as well as economic and environmental features of the process when feedback is present between the liquor recycling and reaction performance. This allowed us to estimate the MSP-RLO and GWP-RLO more accurately than before (see 'Implementing the experimental results in the process model').

Impact of liquor recycling. Guided by the process modelling results, we designed lab-scale RCF experiments that mimic the RCF conditions as obtained from the steady-state simulation. We utilized solvent compositions corresponding to a liquor recycling ranging between 0 and 90%. These compositions are shown in Fig. 3 and summarized in Table S2 (ESI†). We used crude lignin oil from a standard RCF reaction with softwood spruce in these solvent mixtures, as it allowed us to study the monomer formation and stabilization when crude lignin oil is already part thereof, by analysing the syringyl-type monomeric units of the resulting lignin oil, which can only originate from hardwood birch (see Fig. S11, ESI† for a schematic overview). RCF reactions were done in a similar way as for the standard reaction with pure methanol. Typical criteria such as the degree of delignification, monomer yield and carbohydrate retention, and others were used to assess and compare the RCF reactions.

The composition of the carbohydrate pulp obtained with RCF of birch with the applied solvents are depicted in Fig. 6. With pure methanol, 62% of the lignin is extracted whereas most of the hemicellulose (88%) and virtually all cellulose are retained in the pulp. Acetyls have largely been detached from the hemicellulose as signified by a low acetyl retention of 20% (Fig. 6 – MeOH). At 0% liquor recycling, when no crude lignin oil and water are concentrated in the solvent mixture, but methyl acetate is (26 vol%), the pulp is delignified more (80% delignification) than with the pure methanol reaction while it contains a similar amount of hemicellulose and cellulose carbohydrates. Acetyl retention has increased to 30%, which could be assigned to the increasing concentration of methyl acetate in the mixture that can react with free hydroxyl groups of the pulp carbohydrates. For solvent mixtures mimicking a liquor recycling between 25% and 70%, the delignification is higher than the 0% recycle and pure methanol reactions but remains constant at 90%. The hemicellulose retention drops from 82 to 67% whilst most of the cellulose is retained in the pulp (>95%). This trend is continued for the solvent mixture mirroring a liquor recycling of 80%. The wood becomes more delignified, up to 93%, and around 50% of the hemicellulose carbohydrates are removed, whilst most of the cellulose is retained in the pulp. The presence of up to 10 vol% of crude lignin oil in the bulk reaction mixture seems not to have negatively affected the delignification which is, along with the hemicellulose co-extraction, likely promoted by the presence of water in the reaction mixture. This is largely in line with the findings of Jang *et al.* In their work, the delignification (93%) and hemicellulose co-extraction (80%) were promoted using solvent mixtures containing crude lignin oil (8 wt%), methanol and water (at 1 v/v-ratio) whilst they remained constant (56% and 8%, respectively), and comparable to a pure methanol reaction, when only crude lignin oil was enriched – up to 8 wt% – in the methanol solvent. Above 8 wt% crude lignin oil, they also observed an increased delignification likely due to the presence of some water in the solvent mixture.[48] The effect of water,[33,36] seen here already at low concentrations (1–9 vol%), might have been reinforced through the presence of methyl acetate and acetic acid, leading to more acidic conditions in the reaction liquor and consequently, a higher delignification and a larger co-extraction of hemicellulose.[39] This effect seems to be even more pronounced at the highest liquor recycling of 90% when the solvent mixture is highly enriched with crude lignin oil (21 vol%), water (17 vol%), methyl acetate (21 vol%) and acetic acid (3 vol%). In these harsher reaction conditions, 90%

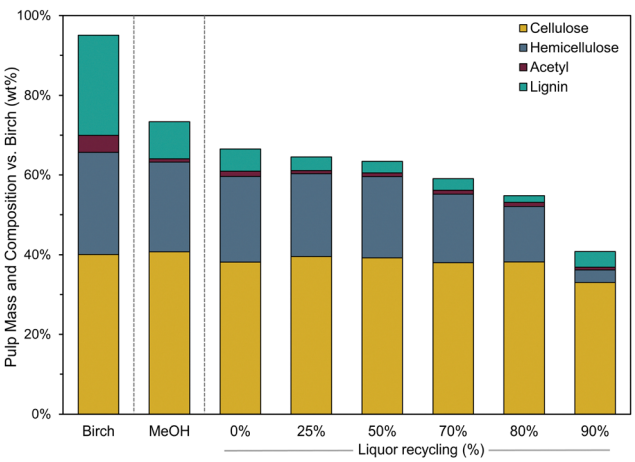

Fig. 6 Pulp mass and composition relative to the birch wood feedstock for RCF with pure methanol (MeOH) and with solvent mixtures comprising methanol, methyl acetate, acetic acid, water and crude lignin oil corresponding to a liquor recycling between 0% and 90%. RCF reactions conditions: 4 g birch sawdust (pre-extracted, particle size 0.25–0.50 mm), 0.4 g of 5% Pd/C, 40 mL solvent (at RT), 220 °C, 30 bar H_2 (at RT) and reaction time of 2 h. The solvent compositions at varying liquor recycling are shown in Fig. 3 and summarized in Table S2 (ESI†). The solvent volume was kept constant to 40 mL (at RT) for all reactions by assuming an CLO density of 0.9 g cm^{-3}, which was modelled by group contribution theory for mixtures of the CLO molecules with Aspen®.

Open Access Article. Published on 02 May 2023. Downloaded on 2/3/2026 7:13:05 AM.
This article is licensed under a Creative Commons Attribution 3.0 Unported Licence.

of the hemicellulose is dissolved and even 20% of the cellulose carbohydrates are removed from the wood. The delignification extent drops slightly to 85% which is likely attributed to lignin oil redeposition on the pulp and not to a decreased lignin extraction from the wood as can be inferred from the resulting lignin oil properties (see below). This suggest that there is an upper limit of the lignin oil concentration with respect to minimizing the lignin content of the carbohydrate pulp.

The results of the pulp compositional analysis show that the delignification is improved with the applied solvent mixtures compared to pure methanol. To examine how these conditions have impacted lignin depolymerization and stabilization, the lignin oil was analysed after removal of sugars, which were traced back in the water-soluble fraction as methylated monomers and/or polyols after liquid–liquid extraction with ethyl acetate and water (Fig. S12, ESI†). Fig. 7A depicts the yield of the syringyl-type monomeric units relative to the birch protolignin (*i.e.*, the S-monomer yield). The S-monomer yield of the lignin oil obtained with RCF mirroring conditions at 0, 25 and 50% liquor recycling is ~5% smaller compared to the RCF reaction with pure methanol (19%). Methyl acetate seems to have adversely affected monomer formation whereas it has promoted lignin extraction, as indicated by the higher degree of delignification for RCF at 0% liquor recycling (78%) compared to the pure methanol reaction (62%). The impact of crude lignin oil seems to be negligible when concentrated to 1 and 2 vol% in the solvent mixture at 25% and 50% liquor recycling, respectively. For the reactions mirroring a high liquor recycling of 70 and 80%, the S-monomer yield has increased to 20% which is comparable to pure methanol RCF. Remarkably, the formation of syringyl type monomers further increases to 24% of the birch protolignin when the solvent mixture contains a large amount of crude lignin oil, namely 21 vol% at 90% liquor recycling. As for the delignification extent, the monomer yield increases when water and acetic acid become more concentrated in the solvent mixture, which is in line with previous reports on the effect of water and acid on the monomer yield in hardwood RCF,[33,39] and it is not adversely affected by the presence of dissolved crude lignin oil. The slightly lower delignification for the 90% liquor recycling reaction seems to contradict this observation. Even though the delignification for this reaction has decreased, the S-monomer yield did not, which prompts us to assume that the dissolved lignin, either originating from the biomass or solubilized in the solvent mixture has redeposited on the pulp rather than that less of the birch protolignin has been extracted and depolymerized. In contrast to reports of Jang *et al.*, monomer formation is not impeded when large amounts of lignin (*i.e.*, more than 4 wt% in their work) are present in the solvent mixture, which they attributed to an increased competition for adsorption on the catalyst surface. Nonetheless, it must be noted that the catalyst in this work is Pd/C instead of Ni/C in theirs. The ability of Pd to assist in the lignin depolymerization through catalytic hydrogenolysis in addition to its hydrogenation capacity stabilizing reactive lignin fragments might explain the higher monomer formation with Pd- than with Ni-catalysis, which is suspected to perform the latter only.[29] This point is currently subject of a more in-depth mechanistic study. In addition, the guaiacyl-type lignin oil of spruce might have a lower tendency to adsorb on the catalyst surface compared to syringyl-type lignin from birch,[76] thereby weakening the effect of lignin enrichment on the catalyst activity, but this hypothesis seems less likely as

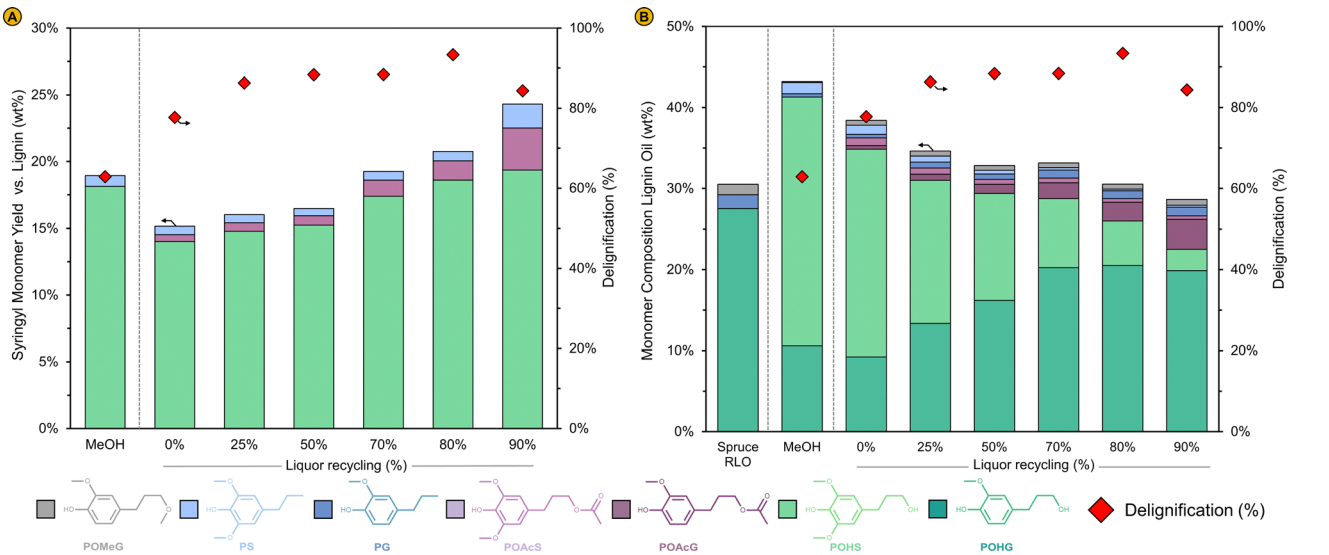

Fig. 7 (A) Monomer yield of the syringyl-type monomeric units *vs.* pristine birch lignin content (left axis) and the degree of delignification (right axis) and (B) monomer composition of the lignin oil (left axis) and the degree of delignification (right axis) for RCF with pure methanol (MeOH) and with solvent mixtures comprising methanol, methyl acetate, acetic acid, water and crude lignin oil corresponding to a liquor recycling between 0% and 90%. The monomer composition of the spruce lignin oil obtained from RCF with pure methanol is also shown and labeled as 'Spruce RLO' (see Material and methods for reaction conditions). The large quantity of G-monomeric units for the lignin oils originates from the spruce crude lignin oil, which was added to the solvent mixture before reaction.

 This journal is © The Royal Society of Chemistry 2023

Open Access Article. Published on 02 May 2023. Downloaded on 2/3/2026 7:13:05 AM.
This article is licensed under a Creative Commons Attribution 3.0 Unported Licence.

substantially more lignin is dissolved in the solvent mixture without showing a detrimental effect compared to their experiments.[48]

As reported earlier, RCF with methanol, a Pd/C catalyst and birch feedstock is highly selective to 4-*n*-propanolsyringol (POHS) with a limited formation of 4-*n*-propylsyringol (PS) and has a comparable monomer selectivity of 44% (Fig. 7B – MeOH). The addition of methyl acetate and/or acetic acid induces the formation of 3-(4-hydroxy-3,5-dimethoxyphenyl) propylacetate, hereafter referred to as 4-*n*-propylacetatesyringol (POAcS), presumably by a partial acetylation of the propanol side chain of POHS. The degree of side-chain acetylation increases for the reactions with more water and acetic acid present – at 70% liquor recycling and above – likely due to an increased acidity of the reaction mixture catalysing the esterification reactions (Fig. 7A). Acetylation of the propanol side chain also occurs with the guaiacyl-type (G-type) monomers. For example, the refined lignin oil obtained with RCF at 0% liquor recycling contains 9% 4-*n*-propanolguaiacol (POHG) and 0.5% 4-*n*-propylacetateguaiacol (POAcG) (Fig. 7B and Fig. S13, ESI†). POAcG becomes increasingly present in the lignin oils obtained with the solvent mixtures containing more spruce crude lignin oil. This signifies that also POHG originally present in the solvent mixture, has been acetylated during RCF of birch wood. Here it is also clearly shown that the spruce lignin oil has been enriched with birch lignin oil given the presence of S-type monomers and the intermediate monomer yields between those of the spruce (30%), and pure birch (43%) lignin oil. At increasing liquor recycling, the total monomer yield of the lignin oils becomes closer to these of the spruce than the birch lignin oil as the contribution of birch lignin to the overall lignin oil weight obviously decreases.

These findings are confirmed by analysis of the refined lignin oils with gel permeation chromatography (GPC), used here to determine the molecular weight (M_w) distribution of the oils. Typical molecular weight distributions of RCF lignin oils containing phenolic monomers, dimers, trimers, and oligomers were obtained which signifies that the depolymerization of lignin and stabilization of reactive monomers has occurred (Fig. S14, ESI†). Given the subtle differences between the various oils, we calculated the number average (M_n) and weight average (M_w) molecular weight from these profiles for comparison (Table 2). The M_n and M_w of the lignin oil for a 0% liquor recycling reaction have increased beyond these of the birch lignin oil obtained with pure methanol (356 g mol^{-1} and 596 g mol^{-1}). The molecular weights of the 25% liquor recycling reactions and higher have also surpassed these of the pristine spruce lignin oil (M_n of 405 g mol^{-1} and M_w of 631 g mol^{-1}). These molecular weight shifts can be explained in multiple ways: (i) a higher delignification of high-M_w lignin combined with (ii) a hindered depolymerization and/or an increased re-condensation might have increased the average molecular weights of the lignin oils between 0 and 50% liquor recycling. The latter seems less likely at 70% liquor recycling and above as S-monomer formation continues to increase for these reactions. Molecular weights might also have increased by (iii) acetylation of both the birch lignin oil, formed during the reaction and the spruce lignin oil, initially added to the solvent mixture. The relatively large presence of acetylated G-type monomers in the lignin oils at high liquor recycling confirms this (Fig. 7B). Hereby, it is possible that also lignin oil dimers and oligomers have been acetylated during reaction, as they have propanol side chains and usually more than one – as shown by detailed molecular analysis of dimers and trimers by Van Aelst *et al.*[43] and Dao Thi *et al.*[77] – available for esterification with acetates. Finally, (iv) recondensation of spruce lignin might also have occurred thereby increasing the molecular weights of the lignin oils, but this was not unambiguously determined here.

Table 2 Number average molecular weight (M_n) and the weight average molecular weight (M_w) of the refined lignin oils for RCF with pure methanol and with solvent mixtures comprising methanol, methyl acetate, acetic acid, water and crude lignin oil corresponding to a liquor recycling between 0% and 90%. The M_n and M_w of the spruce lignin oil obtained from RCF with pure methanol are also shown and labeled as Spruce RLO (see Material and methods for reaction conditions). PDI is the ratio of M_w and M_n and stands for polydispersity index

Lignin oil	M_n (g mol^{-1})	M_w (g mol^{-1})	PDI
Spruce RLO	405	631	1.56
MeOH (birch)	356	596	1.67
0% recycling	396	725	1.83
25% recycling	426	712	1.67
50% recycling	438	731	1.67
70% recycling	463	794	1.71
80% recycling	473	827	1.75
90% recycling	468	820	1.75

Implementing the experimental results in the process model. The experimental results strongly indicate that the process configuration presented earlier (Fig. 2) is technically feasible as RCF continues to work with non-purified solvent mixtures obtained by the liquor and solvent recycle; lignin from the birch wood is extracted and depolymerized thereby producing a carbohydrate pulp and a stable lignin oil rich in phenolic monomers and oligomers. The results also suggest that the RCF reactions with non-purified solvent mixtures will alter the product distribution and properties. Interestingly, more lignin and hemicellulose are extracted from the biomass, resulting in a lignin oil with a somewhat higher M_w, a purer carbohydrate pulp and a larger amount of carbohydrates dissolved in the aqueous product stream. Consequently, the process will have to operate differently as simulated before which implies that a re-evaluation of its technical, economic, and environmental features is necessary. To examine the impact on the technical aspects of the process, the simulations were re-conducted whereby the experimental results for all original liquor recycling rates were used to model the formation of products and consumption of reagents in the reactor. Then, new liquor recycling rates were determined at which the composition and volumetric flow rate of the inlet solvent stream (w/ feedback) matches its original values *i.e.*, as obtained by the simulation with a formation and consumption of products and reagents according to the standard methanol RCF reaction

Open Access Article. Published on 02 May 2023. Downloaded on 2/3/2026 7:13:05 AM.
This article is licensed under a Creative Commons Attribution 3.0 Unported Licence.

(base case). The composition of the make-up solvent has been adjusted in some cases by replacing part of the make-up methanol by water to obtain similar equilibrium concentrations of methanol, methyl acetate, water, and acetic acid. This allowed us to converge the simulation to a new steady state in which the inlet solvent stream composition, and mass formation and consumption in RCF are identical in both the experiments and the process simulation. Following this step, the economic and environmental performance indicators were re-evaluated using the coupled TEA and LCA models. Fig. S15 (ESI†) summarizes these consecutive steps in a schematic way. We did not change economic parameters such as the prices of the pulp and aqueous sugars (fixed at 400 € per t) despite that their intrinsic value might have changed. For example, the value of the pulp could be larger when containing less lignin. As the economics of the RCF biorefinery are highly sensitive for the pulp price (Fig. S16, ESI†), interpreting the results would be less consistent when comparing the lignin oil MSPs which are determined by the capital and operational costs, but also by pulp revenues. Furthermore, it would be too speculative to determine new pulp prices based on lignin content without proving equivalency of RCF pulps with pulps available on the market. These pulps usually have much higher prices, above 1300 € per t.[78]

Fig. 8A and B depict the MSP-RLO and GWP-RLO at various liquor recycling rates for the base case (circles) simulations and the simulations w/ feedback (diamonds). The results are shown in pairs. The labels introduced above in italics, are further used to simplify the description of the results. At a 0% liquor recycling in the base case an identical solvent composition is obtained at 0% liquor recycling w/ feedback, as no crude lignin oil and water are enriched in the solvent mixture. Yet, the MSP-RLO and GWP-RLO decrease as more lignin oil is produced while the capital and operational costs do not change. For the higher recycling rates in the base case, the solvent composition and flow rate match their original values at a lower liquor recycling w/ feedback, and the gap between these recycling rates increases at higher liquor recycling. As the experiments show that more lignin and hemicellulose are extracted from the biomass with the simulated solvent mixtures obtained at a high liquor recycling (w/ feedback) than with pure methanol (base case) the enrichment of a similar amount of crude lignin oil in the solvent mixture occurs already at lower liquor recycling. For example, the solvent composition for a liquor recycling of 25% in the base case corresponds to a solvent composition for a recycling rate of 22.5% w/ feedback, whereas a recycling rate of 80% in the base case, corresponds to 67% w/ feedback. In most of the cases shown here, part of the make-up methanol had to be replaced by water to obtain a similar solvent composition in the simulation as in the experiment as less water is recycled to the reactor (Table S3, ESI†). The feasible range of liquor recycling w/ feedback has also decreased as the design criterion of 10 L kg^{-1} at RT for the solvent-to-biomass ratio is violated already at recycling rates below 90%.

Trendlines were plotted in Fig. 8A and B to reveal the general behaviour of the MSP-RLO and GWP-RLO in function of the liquor recycling when experimental feedback is provided to the process model. Previously showing a linearly, continuously decreasing trend from low to high liquor recycling in the base case (see also Fig. 5), the MSP-RLO and GWP-RLO now bend-off at high liquor recycling w/ feedback. At low liquor recycling, the estimated MSP-RLO and GWP-RLO w/ feedback are lower compared to base case as more lignin oil is produced whilst a similar liquor recycling rate can be maintained. This gap, between the MSP and GWP estimates of the base case and w/ feedback, decreases with increasing liquor recycling as the

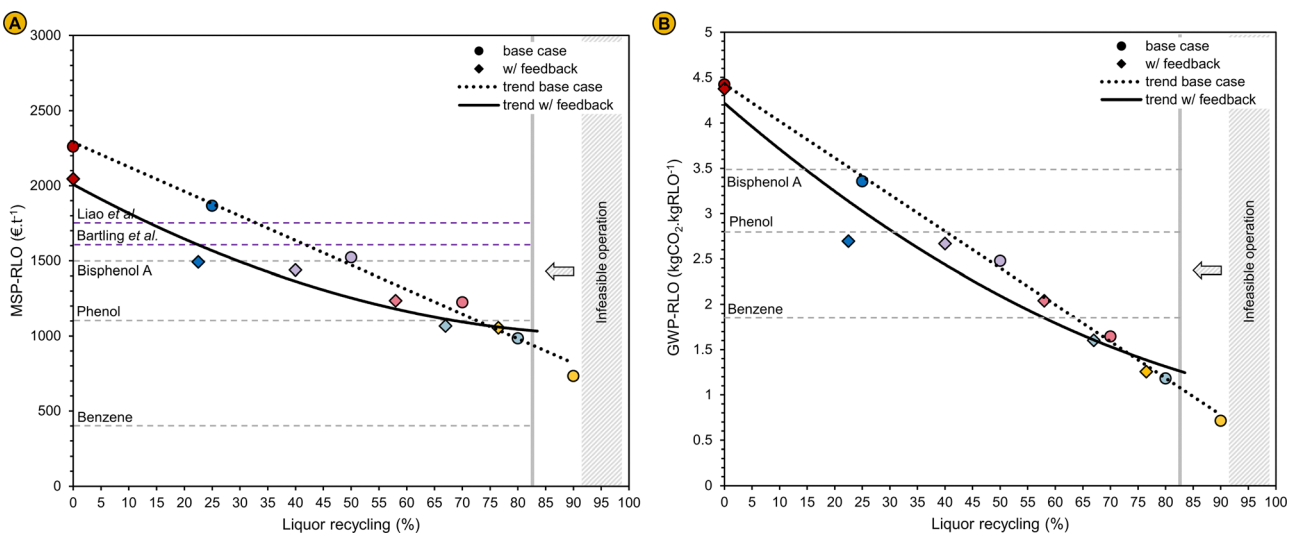

Fig. 8 (A) MSP-RLO and (B) GWP-RLO in function of the liquor recycling. The liquor recycling in the base case *i.e.*, with a formation and consumption of products and reagents according to the standard pure methanol RCF reaction are represented by the circles and the trends are shown by the dotted lines (base case) – see also Fig. 5. The liquor recycling obtained when experimental results are implemented in the process simulation are represented by the diamonds and the trends are shown by the solid lines (w/ feedback). Pairs for which the solvent composition matches in both instances are given the same colour. The liquor recycling rates of the pairs are tabulated in Table S3 of the ESI.†

 This journal is © The Royal Society of Chemistry 2023

Open Access Article. Published on 02 May 2023. Downloaded on 2/3/2026 7:13:05 AM. This article is licensed under a Creative Commons Attribution 3.0 Unported Licence.

lignin oil productivity plateaus as was shown experimentally (Fig. 7). The additional benefit of a larger lignin extraction with the solvent mixtures at these higher liquor recycling rates diminishes. As result, the trendlines coincide at a liquor recycling of ~75%. Above 80% liquor recycling w/ feedback, the operation becomes infeasible due to a violation of the solvent-to-biomass design criterion of 10 L kg^{-1} at RT (see 'Operation of the liquor recycle system'). The estimates of these performance indicators show that liquor recycling remains a useful strategy to improve the economics and sustainability of the RCF biorefinery process. The MSP-RLO and GWP-RLO are still competitive compared to fossil-based analogues like phenol and BPA.

Reducing the reactor capital costs

Univariate analysis of reaction conditions. Like Bartling *et al.*, we also found that the high-pressure reactor system is the largest contributor to the total capital expenditure (Fig. 4B). The high reactor costs can be attributed to the inherently-slower kinetics of the lignin extraction and solvolysis in RCF[30,79] requiring much larger processing volumes compared to smaller unit operations downstream, where mass transfer is generally faster. Therefore, the MSP-RLO can be significantly reduced by diminishing the reactor capital costs. These costs are determined by multiple technical variables that directly impact the reactor sizing and shell mass such as the solvent composition and loading, the residence time and the reactor temperature and pressure. We already showed that the reactor size and costs can be reduced by using less volatile solvent mixtures, limiting the volumetric expansion at the constant reactor conditions of 220 °C and 90 bar, when the process is operated with a high liquor recycling (Fig. 3 and 4B). However, we expect the reactor residence time and reaction temperature to have an even larger impact on the reactor costs than the liquor recycling. This is shown by the univariate analysis of reactor residence time (±1 h) and reaction temperature (±20 °C) (Fig. S17, ESI†). The analysis shows that the MSP-RLO can be further reduced by up to 15% for a liquor recycling of 80% (base case) when changing the reactor residence time from 2 to 1 h – thereby essentially halving the reactor volume. The MSP-RLO also changes substantially with the reaction temperature. The percentage change amounts −8% when the reaction temperature is lowered from 220 °C to 200 °C as the reactor vessels walls can be thinner. However, RCF kinetics are slower at lower temperature which might offset any economic gains. For both the reaction time and reactor residence time, the benefits of a lower capital expenditure do not necessarily outweigh the losses associated with reduced lignin oil yields and lower product sales. Typical trade-offs like these are not considered in this univariate analysis as it is assumed that the RCF reaction is not affected by the changing reaction conditions.

Optimization of reaction conditions. To identify these trade-offs, we conducted RCF experiments at lower reaction time and temperature with a solvent mixture corresponding to an 80% liquor recycling (base case). The process economics and sustainability were then re-evaluated by implementing the experimental results in the simulation as was done previously (see 'Implementing the experimental results in the process model') and by adjusting the model parameters related to the reactor capital costs as was done in the univariate analysis. This allowed us to estimate the impact of time and temperature more accurately than before.

The delignification extent decreases from 93% to 81% and the hemicellulose retention increases from 54% to 69%, respectively, when the residence time for this RCF reaction is halved from 2 h to 1 h at a reaction temperature of 220 °C. Although substantially more lignin is extracted from the biomass at these conditions compared to the RCF reaction with pure methanol (62% delignification), less monomers are formed as shown by the reduced S-monomer yield, which decreases from 21 to 14%, below the S-monomer yield of a pure methanol reaction (19%) (Fig. 9A and B). Likely, the lignin extracted from the wood matrix has not been depolymerized fully after 1 h of reaction time, suggesting that the lignin extraction rate might be larger than the rate of depolymerization with this reaction system and at these conditions. This is confirmed by GPC analysis of the lignin oil. The M_n (483 g mol^{-1}) and M_w (873 g mol^{-1}) are larger than at a reaction time of 2 h (473 and 827 g mol^{-1}) implying that depolymerization is incomplete. Reducing the reaction temperature to 200 °C has a similar effect on the RCF performance metrics as halving the reactor residence time: less lignin is extracted (70% delignification) but the delignification remains larger than that of a pure methanol reaction, and the S-monomer yield (11%) is smaller compared to the reaction at 220 °C and decreases to below the monomer yield of pure methanol RCF. The M_n (472 g mol^{-1}) and M_w (850 g mol^{-1}) are comparable with the RCF reaction at 220 °C. The hemicellulose retention has also increased, to 78%. For both reactions, deacetylation of the hemicellulose has decreased somewhat (~10%) compared to the reaction at 220 °C and 2 h, likely due to an increased hemicellulose retention. The GC and GPC spectra of the lignin oil and the GC spectrum of the aqueous phase are depicted by Fig. S18–S20 in the ESI.†

The economics and sustainability for the RCF biorefinery systems with a lower reactor residence time and reaction temperature were re-evaluated after implementation of the experimental results in the process simulation. Liquor recycling rates and the make-up solvent composition were adjusted from the initial 80% to match the inlet solvent composition of the simulations with the solvent composition used in experiments as closely as possible (Fig. S21, ESI†). It must be noted that the lower deacetylation of the wood at the lower reaction time and temperature has led to a somewhat lower concentration of methyl acetate in the solvent composition in the simulations than used in the experiments as the make-up solvent was only modified by addition of water. However, these differences are limited and not expected to impact the reaction performance substantially as can be inferred from previous experiments (see 'Impact of liquor recycling').

As expected, the reactor capital costs decrease from 87 M€ for the 220 °C–2 h case to 50 M€ for the 220 °C–1 h case and to 60 M€ for the 200 °C–2 h case (Fig. 9C). The capital costs for

Open Access Article. Published on 02 May 2023. Downloaded on 2/3/2026 7:13:05 AM.
This article is licensed under a Creative Commons Attribution 3.0 Unported Licence.

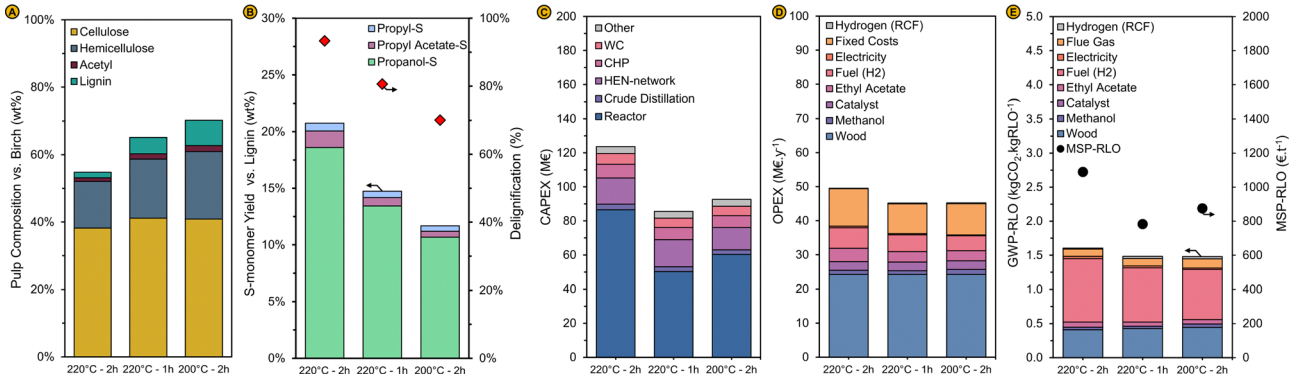

Fig. 9 (A) Pulp mass and composition relative to the birch wood feedstock and (B) monomer yield of the syringyl-type monomeric units *vs.* pristine birch lignin content (left axis) and the degree of delignification (right axis) for RCF reactions with varying reaction time and temperature. The solvent composition for these reactions is shown in Fig. S21 (ESI†). Standard reaction conditions, except for time and temperature, were used (see caption Fig. 6). (C) capital costs distribution (D) operational costs distribution and (E) GWP-RLO (left axis) and MSP-RLO (right axis) for the process operating at varying RCF reaction time and temperature. The modelling results are obtained by re-implementation of the experimental results in the process simulation (see 'Implementing the experimental results in the process model').

distillation and the CHP also decrease as the liquor recycling can be set higher to 73% and 76%, respectively, instead of 67% before a similar composition is attained at the inlet solvent stream due to the lower (crude) lignin oil productivity in both reactions (Fig. 9B). This also impacts the fuel costs required for distillation and the ethyl acetate purchasing costs. Less liquid is distilled, and less ethyl acetate is consumed in the liquid–liquid extraction due to the lower crude lignin oil production. Operational costs also decline in both cases as the fixed costs of production (*e.g.*, maintenance, property tax, *etc.*), which are partially estimated based on the capital costs, decrease (Fig. 9D). Despite a lower lignin oil productivity, these costs reductions are significantly large enough to decrease the lignin oil selling price and carbon footprint. The MSP-RLO declines from 1089 to 784 and 875 € per t for the 1 h and the 200 °C case, respectively. The GWP-RLO drops slightly from 1.60 to 1.48 and 1.47 $kgCO_2\ kgRLO^{-1}$ (Fig. 9E). As discussed in previous section, economic parameters such as the pulp and carbohydrate pricing were kept constant in these MSP-RLO and GWP-RLO calculations to examine the impact on lignin oil independently (see 'Implementing the experimental results in the process model'). In general, this analysis shows that the technical variables (*viz.*, reaction time, temperature, liquor recycling, *etc.*) are strongly interdependent and all impact the economics and environmental impact of the RCF biorefinery.

General applicability of the process design

Any future biorefinery should be able to operate flexibly and respond to changing external, economic circumstances. One essential feature is that, like current petroleum refineries processing various types of oil, the RCF biorefinery should be able to process different types of wood feedstocks. In previous sections, an integrated analysis of the RCF biorefinery processing a hardwood feedstock, namely birch with a moisture content of 15 wt%, was presented. As illustration, we show here that this biorefinery process is technically capable of processing two other feedstock types *viz.*, (i) a softwood spruce with a 15% moisture content and, (ii) a hardwood birch with a moisture content of 30%, double the amount of what was previously assumed.

Softwood *vs.* Hardwood. In general, softwoods differ from hardwoods in two ways by which the biorefinery process is affected. First, softwoods contain more lignin – up to 28 wt% – and the lignin is less easily extracted from the wood matrix as shown previously by Van den Bosch *et al.*[17] This might result in a lower crude lignin oil concentration in the solvent mixture at high liquor recycling. Second, softwoods generally have less acetyl-groups attached to the hemicellulose – usually less than 1 wt% – compared to hardwoods.[80] This will reduce the acetate concentration in the solvent mixture. These presumptions are confirmed by an RCF reaction with a softwood spruce in pure methanol at similar reaction conditions as for the birch feedstock (*i.e.*, 220 °C, 2 h, 10 L kg^{-1}). The degree of delignification amounts 40% and the monomer selectivity of the lignin oil is 34%. Deacetylation of the spruce feedstock occurs. Methyl acetate is detected in the impurified RCF reaction liquor but to a lesser extent as for a similar reaction with birch (Fig. S4b, ESI†). In addition, all cellulose and most of the hemicellulose (82%) is retained in the pulp (Fig. 10A and B – MeOH). Following this standard RCF reaction, the same procedure as described in previous sections of this work was applied to examine the impact of liquor recycling on the RCF biorefinery, its economics and environmental footprint (Fig. S15, ESI†). The solvent mixture at high liquor recycling is still enriched with methyl acetate (12 vol%), water (8 vol%), acetic acid (0.4 vol%) and crude lignin oil (9 vol%) but as expected, it contains less acetates and crude lignin oil compared to the solvent mixture obtained with birch at a similar liquor recycling rate of 80%, as simulated without experimental feedback (Fig. 11A and Fig. S22a, ESI†). Comparable to the reactions with birch, this solvent mixture enhances the spruce lignin extraction (57%) whilst producing a higher-M_w lignin oil (M_n of 496 and M_w of 733), which is partially acetylated, compared to a pure MeOH reaction with spruce (Fig. 10A – 80% recycle). The GC and GPC

 This journal is © The Royal Society of Chemistry 2023

Open Access Article. Published on 02 May 2023. Downloaded on 2/3/2026 7:13:05 AM.
This article is licensed under a Creative Commons Attribution 3.0 Unported Licence.

spectra of the lignin oil and the GC spectrum of the aqueous phase are shown in Fig. S18–S20 (ESI†).

The capital and operational costs of the RCF biorefinery processing spruce are fairly similar to the comparable case with birch. Capital costs amount 123 M€, with the reactor being the largest cost contributor (87 M€) and the operational cost amount 49 M€ per year whereby some costs (*e.g.*, the methanol and ethyl acetate purchasing costs) are smaller and others (*e.g.*, fuel costs) are larger when using spruce feedstock due to small differences in the operation of the refinery. On one hand, less ethyl acetate and methanol are required for the crude lignin oil extraction and solvent make-up, respectively, as the crude lignin oil productivity is lower, and less methanol is consumed in a spruce RCF reaction. On the other hand, more fuel is needed due to the larger concentration of methanol (67 *vs.* 51 wt%) in the distillation inlet stream (Fig. S23a, ESI†) which has a similar flow rate for the spruce and birch case given the comparable liquor recycling rate (69% and 67.5%) obtained after reimplementation of the experimental results. Due to the lower lignin oil production in RCF, the MSP-RLO is higher for the spruce (1228 € per t) than for the birch (1089 € per t) case. The increased GWP-RLO for spruce (1.88 $kgCO_2$ $kgRLO^{-1}$) compared to birch (1.60 $kgCO_2$ $kgRLO^{-1}$) is explained in a similar way as the operational costs (Fig. 11B).

Biomass moisture content. Wood feedstocks supplied to a biorefinery may have varying moisture contents which are preferably adjusted to a fixed value before entering the process. Reducing the moisture content of the wood to low levels might be expensive[69] which makes it interesting to examine how an increased moisture content impacts the RCF biorefinery. A similar procedure as used before was applied to model an RCF biorefinery based on the identical process design that uses

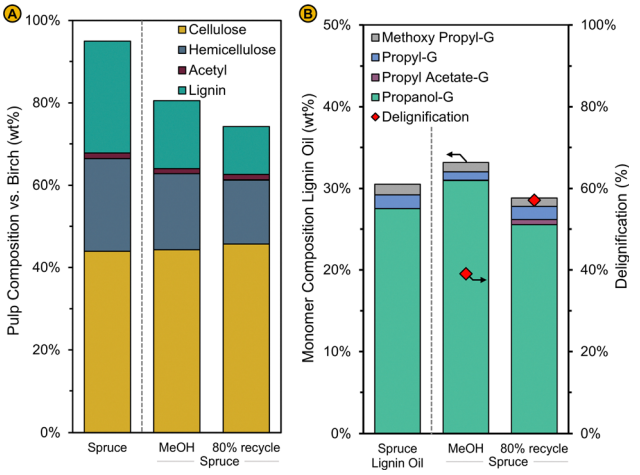

Fig. 10 (A) Pulp mass and composition relative to the spruce wood feedstock (Spruce) and (B) monomer composition of the lignin oil (left axis) and degree of delignification (right axis) for an RCF reaction with pure methanol (MeOH) and for a RCF reaction with solvent composition corresponding to a liquor recycling rate of 80% in the base case (80% recycle). The solvent composition for this reaction is shown in Fig. 11a. Standard reaction conditions (220 °C, 2 h, 10 L kg^{-1}) were used in these spruce RCF reactions (see also caption Fig. 6).

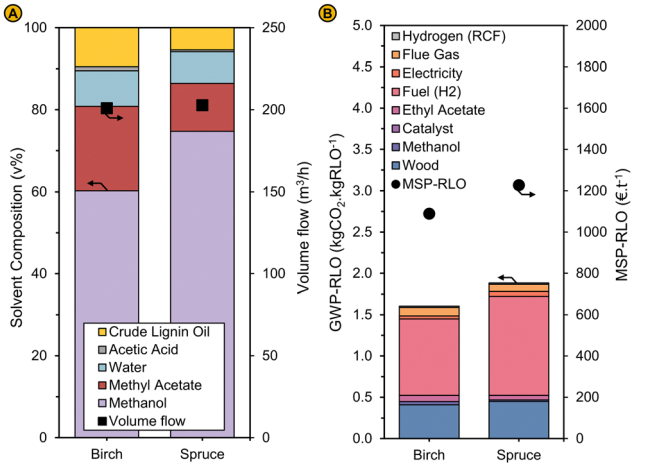

Fig. 11 (A) Solvent composition (left axis) and volumetric flow rate (right axis) (B) GWP-RLO (left axis) and MSP-RLO (right axis) for the RCF process using birch and spruce as feedstock and using a solvent mixture in RCF modelled at a liquor recycling of 80% in the base case. The modelling results shown here are obtained by reimplementing the experimental results (see Fig. 10) in the process simulation (see 'Implementing the experimental results in the process model'). An identical feedstock price was used for spruce as for birch.

feedstock with a moisture content of 30% (Fig. S15, ESI†). As anticipated, the increased moisture content of the wood feedstock increases the water concentration in the solvent mixture already at low liquor recycling (Fig. S22b, ESI†). Fig. 13 depicts the solvent composition for birch with a moisture content of 15% (15% MC) and 30% (30% MC), when the liquor recycling is set to 80% at first and then adjusted to 68% and 64%, respectively along with the make-up solvent composition after reimplementation of the experimental results. Less methyl acetate is concentrated in the solvent due to an increased formation of acetic acid which does not concentrate in the recycle loops as it primarily leaves the RCF area *via* the bottoms of the crude distillation column to the liquid–liquid extractor due to its high boiling point. The degree of delignification (95%) is similar to the case with a 15% MC (93%), but more hemicellulose sugars are removed (retention of 33%), likely because more water is present in the solvent mixture (Fig. 12A). The S-monomer yield for the 30% MC reaction amounts 16%, which is below the yield of the pure methanol reaction (19%) and the reaction mirroring 15% MC (21%) (Fig. 12B). Interestingly, the M_n (467 g mol^{-1}) of the 30% MC reaction is comparable to the reaction with a 15% MC, but the M_w (718 g mol^{-1}) is lower, resulting in an overall lower polydispersity (1.54 *vs.* 1.75). Despite the smaller yield of S-type monomers, less high-M_w lignin seems to be present in this lignin oil, which could point at an increased depolymerization of higher-M_w lignin, either from the birch feedstock or the original spruce lignin oil, added to mimic the solvent mixture. We did not investigate these hypotheses systematically in this work and leave this open to discussion. The GC and GPC spectra of the lignin oil and aqueous phase are depicted by Fig. S18–S20 in the ESI.†

Open Access Article. Published on 02 May 2023. Downloaded on 2/3/2026 7:13:05 AM.
This article is licensed under a Creative Commons Attribution 3.0 Unported Licence.

The economics and environmental footprint of the process were re-evaluated using the TEA and LCA models after implementation of the experimental results in the process simulation and readjustment of the liquor recycling and the make-up solvent composition. The reactor capital costs are substantially smaller for the case with 30% MC (77 M€) than for 15% MC (87 M€) as the solvent mixture entering the reactor is less volatile due the larger presence of water. This leads to an overall lower capital cost of 114 M€ for the 30% MC *vs.* 124 M€ for the 15% MC case. Operational costs are mainly impacted by the larger fuel requirements (7.1 *vs.* 6 M€ per year) for removing methanol from the distillation inlet stream which contains more water, and the increased purchasing costs for ethyl acetate (5.4 *vs.* 3.9 M€ per year) which is lost more to the aqueous stream due to the larger amounts of water entering the liquid–liquid extraction. In this case, it might be interesting to adjust the amount of water before entry in the extractor to reduce these losses, but only if that leads to improved economics of the process. The operational costs for the 30% MC (53 M€ per year) have increased by 3 M€ per year compared to the similar case with 15% MC (50 M€ per year). The reduced capital costs and increased operational costs lead to an estimated MSP-RLO that is similar in both cases. The MSP-RLO amounts 1113 € per t for the 30% MC case which is just 46 € per t more than the estimate of 1089 € per t for 15% MC. The GWP-RLO has increased from 1.60 to 1.89 $kgCO_2$ $kgRLO^{-1}$, which is mainly due to the larger fuel and ethyl acetate intake (Fig. 13B). Importantly, we did not alter the price or global warming potential of the wood feedstock even though this might be required for woods with a higher moisture content. The cost and carbon footprint could be larger due to the transportation of heavier wood. However, as the drying of wood is a large contributor (20%) to the feedstock price,[69] it can be expected that the MSP-RLO can be further reduced when using wood with a larger moisture content.

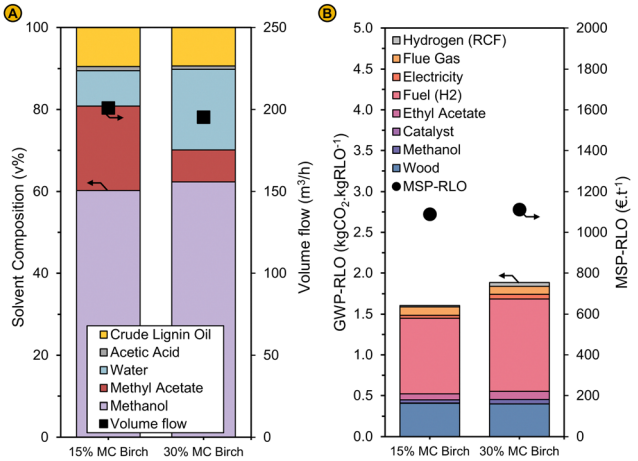

Fig. 13 (A) Solvent composition (left axis) and volumetric flow rate (right axis) (B) GWP-RLO (left axis) and MSP-RLO (right axis) for the RCF process using birch feedstock containing 15% moisture (15% MC birch) and 30% moisture (30% MC birch) and using a solvent mixture in RCF modelled at a liquor recycling of 80% in the base case. The modelling results are obtained by reimplementing the experimental results (see Fig. 12) in the process simulation (see 'Implementing the experimental results in the process model').

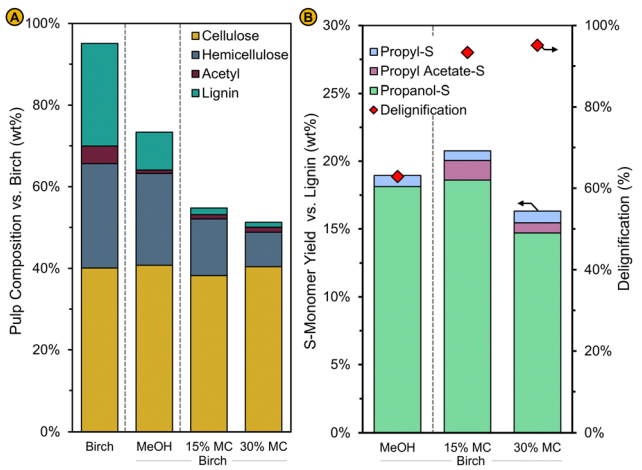

Fig. 12 (A) Pulp mass and composition relative to the birch wood feedstock (Birch) (B) monomer yield of the syringyl-type monomeric units *vs.* pristine birch lignin content (left axis) and the degree of delignification (right axis) for an RCF reaction with pure methanol (MeOH) and for an RCF reaction with solvent composition corresponding to a liquor recycling rate of 80% obtained for the birch feedstock containing 15% moisture (15% MC) and 30% moisture (30% MC). The solvent composition for these reaction is shown in Fig. 13a. Standard reaction conditions were used (see caption Fig. 6).

Conclusions

This work presents a novel reductive catalytic fractionation (RCF) biorefinery process in which RCF (by-)products, including the lignin-derived bio-oil, are partially recycled to the reactor along with the solvent methanol resulting in significantly improved economics and a more sustainable biorefinery operation as indicated by minimum selling price (MSP-RLO) and global warming potential (GWP-RLO) of the lignin oil. The results of this work are summarized in Fig. 14.

Unique solvent mixtures comprising (i) methanol, (ii) methyl acetate and (iii) acetic acid, formed by deacetylation of hemicellulose, (iv) water, released from the wood matrix and, (v) the crude lignin oil, were obtained by partially returning the RCF reaction liquor to the reactor before a crude distillation step (*i.e.*, liquor recycling) and by allowing reaction by-products such as methyl acetate to concentrate in the solvent recycle loop following a crude distillation step to remove the crude lignin oil and excess water (*i.e.*, solvent recycling).

Simulation of this RCF biorefinery process at multiple steady-state operations whereby the liquor recycling percentage was systematically varied showed that the process economics and CO_2 footprint can be significantly improved in this way as excessive solvent distillation is avoided. This proof-of-concept process model was corroborated by and adjusted with the results of lab-scale experiments that mimic the newly simulated RCF solvent mixtures. It was demonstrated that by using solvent mixtures containing methanol, methyl acetate, water,

 This journal is © The Royal Society of Chemistry 2023

Open Access Article. Published on 02 May 2023. Downloaded on 2/3/2026 7:13:05 AM.
This article is licensed under a Creative Commons Attribution 3.0 Unported Licence.

acetic acid, and crude lignin oil (to up to 20 vol%) – as simulated for a high liquor recycling – the lignin extraction is enhanced, the monomer yield remains high, and the hemicellulose co-extraction is promoted. This leads to an overall lower MSP-RLO and reduces the GWP-RLO significantly, levelling the selling price of phenol and the GWP of benzene (Fig. 14 – Liquor recycling).

The RCF biorefinery economics were optimized further by lowering the reactor capital costs which was achieved by reducing the reactor residence time and reaction temperature for a solvent mixture at high liquor recycling. Despite the somewhat lower lignin oil productivity at these 'milder' conditions, the MSP-RLO could be further reduced to below the price of phenol (Fig. 14 – Reactor cost optimization).

Finally, the general applicability of this process concept was demonstrated by applying the modelling and experimental procedures developed in this work to different feedstocks. The process remains functional *i.e.*, the recycle system proves useful when switching from hardwood to softwood but the composition of the solvent mixtures at varying liquor recycling changes. When using spruce instead of birch, the solvent mixtures contain less acetates and crude lignin oil, given the lower productivity of these compounds in the RCF reaction. In line with the birch case, the lignin oil yield is enhanced when liquor recycling is applied leading to a spruce MSP-RLO levelling the phenol selling price and GWP-RLO equal to benzene (Fig. 14 – Spruce feedstock). It was also shown that woods with a higher moisture content can be processed by the biorefinery whilst maintaining a similar MSP-RLO and GWP-RLO as the corresponding case with lower moisture content (Fig. 14 – 30% MC birch). Overall, the methodologies developed in this work can be further applied to optimize the reaction conditions, explore other feedstock types as well as other solvent systems in developing an economically feasible and environmentally sustainable lignin-first RCF biorefinery.

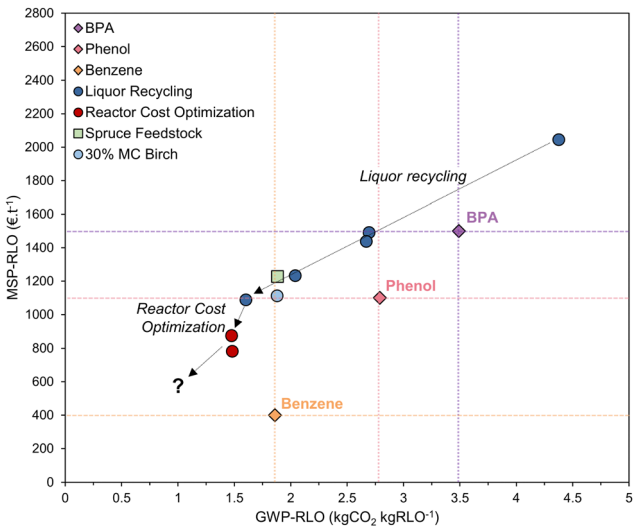

Fig. 14 Global warming potential (GWP-RLO) *vs.* minimum selling price (MSP-RLO) of the lignin oil for all cases examined in this work. The GWP-RLO represents the scenario where no renewable energy vectors (*i.e.*, renewable hydrogen and electricity) were used in the RCF biorefinery and the carbon neutrality principle was not applied. This allows to better compare the gains achieved with liquor recycling and reactor cost optimization compared to the GWP of fossil-based chemicals. GWPs are on average 2 to 4 times smaller when renewable energy resources are used and decrease by $\sim$5 $kgCO_2$ $kgRLO^{-1}$ under the carbon neutrality principle (see 'Global warming potential of the lignin oil').

Materials and methods

Process simulation

Component definition, property methods and property estimation. Process simulations were conducted in Aspen HYSYS® process simulation software. Crude lignin oil components *viz.*, the lignin oil phenolics, methylated sugars and extractives were not originally present in the Aspen HYSYS component database, hence, were defined as hypothetical components for which thermodynamic and physical properties were estimated using UNIFAC group contribution methods using a built-in molecule generator. Six monomers, two oligomers, mirroring the G- and S-type phenolics and two methylated sugar monomers (C5 and C6) were defined as hypothetical components representing the crude lignin oil using this method. Acetylated equivalents of the lignin oil components were defined to confirm their expected behaviour in the process simulation. The binary interaction parameters were estimated using the UNIFAC correlations which were fit to the NRTL-SRK activity coefficient model which was used given the non-ideality of the systems under consideration. The molecular structures of the hypothetical components are depicted in Fig. S24 of the ESI.†

Aspen energy analyser and CHP calculations. Aspen Energy Analyzer® was used for basic heat integration of the process heaters and coolers *via* pinch point analysis to estimate net heating and cooling requirements of the process. The minimum and maximum temperatures of process streams were confined between 40 and 249 °C, respectively, to avoid using refrigerants and fuel oils for cooling and heating, respectively. The total electricity consumption was estimated from the process pumps and compressors and the cooling water pump around, obtained from the energy optimization, for which a typical power consumption of 1.5 kWh/3.8 m^3 was employed.[81] Gas turbine and steam boiler calculations were then completed in a python-based model using the utilities data from Aspen Energy Analyzer and the process purge and off-gas stream properties obtained with the Aspen HYSYS simulation. A steam system containing a high (at 250 °C), medium (at 175 °C) and low (at 125 °C) pressure steam cycle was modelled following a methodology presented by Nieuwlaar *et al.*[82] In this way, a net input of additional fuel and electric power could be estimated. Fig. S5 (ESI†) gives a schematic overview of the CHP model. The parameters (*viz.*, turbine efficiency, boiler efficiency, condensate return, *etc.*) used in the calculations are presented in Table S4 (ESI†).

Techno-economic assessment

Factorial cost estimation. The capital expenditures were estimated using the factorial cost estimation method. Sizing

Open Access Article. Published on 02 May 2023. Downloaded on 2/3/2026 7:13:05 AM. This article is licensed under a Creative Commons Attribution 3.0 Unported Licence.

parameters of the reactor and unit operations were (in)directly obtained from the Aspen HYSYS simulation and the sizing parameters of the heat exchangers were estimated by the Aspen energy analyzer. Reactors were modelled as jacket agitated vessels based on their volume which was estimated from the volumetric flowrate of the reactor outlet at reaction temperature and the reactor residence time. The reactor equipment costs at higher and lower temperature than the base case simulation (at 220 °C) in the univariate analysis were calculated using a pressure-dependent scaling factor that was obtained by the cost simulation of pressure vessels over a range between 40 and 120 bar (Fig. S25, ESI†). The pressures at 200 and 240 °C were modelled to maintain a constant volumetric flow rate, in this way, only the thickness of the reactor vessel is affected and not the total reactor volume. Stainless steel material ss316 was used for the reactor section, crude oil distillation and recycle system, but not for the crude oil purification unit operations. Costs of the CHP were modelled using an overnight capital cost of 950 € per kW for the gas turbine[83] and the steam boiler cost equation used in the factorials method. Costs were escalated using appropriate cost escalation indices and converted to European pricing by multiplication with a European averaged location factor of 1.11 and a currency rate of 0.9 € per $. A list with detailed economic parameters is presented in Table S5 of the ESI.†

Operational costs. Operational costs were determined by the variable costs of the raw materials, consumables, utilities which were obtained from the process simulation and CHP calculations and the fixed costs of production (*i.e.*, salaries, overheads, property tax, environmental costs, *etc.*). Pricing of the raw materials, consumables, utilities and products are shown in Table S6 (ESI†). Wood feedstock price was set to 158 € per t as previously estimated by Liao *et al.* Pulp and aqueous sugars are sold for a 400 € per t price, following an average sugar price.[69]

Minimum selling price. The minimum selling price was solved for the net present value (NPV) of the project to be zero using a weighted average cost of capital of 15%. The project lifetime was set to 20 years and a capital depreciation period of 10 years was used in a straight-line depreciation procedure. A comprehensive list of economic parameters is provided in Table S5 (ESI†).

Life cycle analysis

Global warming potential. The global warming potential for the production of 1 kg of refined lignin oil was estimated for a cradle-to-gate system boundary. A diagram of the LCA-scope can be found in Fig. S7 (ESI†). Process in- and outputs of the RCF biorefinery were simulated with the Aspen HYSYS process simulation. Life cycle inventories of the background technologies and production processes for the refinery in- and outputs were obtained from Ecoinvent v3.8 and Thinkstep Gabi professional database to determine their environmental impact. The production processes and corresponding GWP values for each of the in- and outputs are listed in Table S7 (ESI†). Biogenic carbon uptake and emission were only considered for those biogenic carbon streams, for which appropriate characterization factors could be estimated. For example, process CO_2 emissions from biogenic origin like the acetyl combustion in the CHP were accounted for in the GWP calculations by using a characterization factor of 0.2, assuming a birch rotation time of 50 years, and biogenic carbon life time of 0 years as it is directly combusted at the refinery level.[75] Biogenic carbon that ends up in the refinery products (*viz.*, lignin oil, pulp and aqueous sugars) was not included in the GWP calculations to avoid having to estimate appropriate product life times. Economic allocation based on product and by-product revenues was used to assign CO_2 emissions to the refined lignin oil for which a fixed price of 1500 € per t was used. GWP values were calculated for a 100 year time scale and expressed in kg of CO_2 equivalent.

Tabulated data of all figures can be found in the Tables section of the ESI† (Tables S8–S33).

Experimental methods

RCF reaction. RCF experiments were performed in a 100 mL batch reactor (Parr Instruments Co.). In a typical experiment, 4 g of birch (Betula pendula), 0.4 g of catalyst (5 wt% Pd/C) and 40 mL of solvent were loaded in the reactor which is pressurized to 30 bar with H_2 after being flushed with N_2. The reactor is heated to 220 °C, at $\sim$10 °C min^{-1} at which the total pressure reached $\sim$60 to 80 bar. The reactor was cooled with water and depressurized at RT after the reaction.

Chemical analysis. The in- and outputs of the reactor were analysed using multiple experimental procedures. A brief overview of these procedures is described here. The reader is referred to Section 1 of the ESI† for a more detailed description. The reactor content was filtered to yield a carbohydrate pulp and a liquid crude lignin oil which was subject to a threefold liquid–liquid extraction with ethyl acetate and water to produce a refined lignin oil (after EtOAc evaporation) and a water-soluble fraction containing sugar derivatives. The carbohydrate pulp composition was determined using a standard total sugar procedure[84–86] combined with a standard procedure for carbohydrate and lignin analysis.[87] The lignin content was analysed by weighing the Klason lignin obtained after filtering the pulp hydrolysate whose UV-absorbance was measured at 240 nm for acid-soluble lignin determination. Acetyl content of the pulp was analysed by HPLC of the hydrolysate from which the sugars were analysed by GC as alditol acetates following a derivatization procedure. A similar procedure was followed for the birch compositional analysis. Refined lignin oil components were derivatized *via* trimethylsilylation with *N*-methyl-*N*-(trimethylsilyl)trifluoroacetamide, to increase their volatility before GC analysis. An internal standard 2-isopropylphenol was added to the refined lignin oil for quantitative analysis. GC/MS was used for chemical analysis of the phenolic monomers. Gel permeation chromatography (GPC) was used to confirm the presence of phenolic monomers, dimers and higher oligomers. The sugar speciation of the water-soluble fraction was determined in a similar way, *via* trimethylsilylation, but with a different internal standard, myo-inositol, which was added after evaporation of the water. Both GC and GC/MS were used

 This journal is © The Royal Society of Chemistry 2023

to qualitatively examine these sugars. The gas phase was analysed by GC.

Conflicts of interest

There are no conflicts to declare.

Acknowledgements

The authors would like to thank Ben Wambacq and Giel Dreezen for their help with providing the spruce crude lignin oil, used in the experiments presented in this work. The authors would also like to thank Kranti Navare for her input on the life cycle assessment. W. A. and B. S. thank internal funding from KU Leuven (IDN project – FFASSD, IDN/19/023) for supporting this research. B. S. acknowledges funding from VLIR through the iBOF project Next-BIOREF (iBOF/21/105). S. V. d. B. and J. V. A. acknowledge Flanders Innovation & Entrepreneurship (Innovation Mandate, VLAIO/HBC.2019.2187) and the Industrial Research Fund of KU Leuven (IOF Mandate, IOFM/20/006; C3-project – BIOCON, C3/19/015) and also acknowledge the funding received from the Bio Based Industries Joint Undertaking under the European Union's Horizon 2020 research and innovation programme with grant agreement no. 837890 (SMARTBOX) and the funding received from the Flemish Government under the Vlaamse Veerkracht relance plan (VV023/02) supported by the European Union (NextGenerationEU). K. V. A. acknowledges funding through FWO-SBO project BioWood (S003518N). E. C. acknowledges funding through FWO-EoS project BIOFACT (G0H0918N).

Open Access Article. Published on 02 May 2023. Downloaded on 2/3/2026 7:13:05 AM.
This article is licensed under a Creative Commons Attribution 3.0 Unported Licence.

Notes and references

1 M. Carus, L. Dammer, A. Raschka, P. Skoczinski and C. Berg, Renewable carbon is Key to a Sustainable and Future-Oriented Chemical Industry, **www.bio-based.eu/nova-papers**.
2 J. P. Lange, *Energy Environ. Sci.*, 2021, **14**, 4358–4376.
3 P. N. R. Vennestrøm, C. M. Osmundsen, C. H. Christensen and E. Taarning, *Angew. Chem., Int. Ed.*, 2011, **50**, 10502–10509.
4 P. Gallezot, *Chem. Soc. Rev.*, 2012, **41**, 1538–1558.
5 J. S. Luterbacher, D. Martin Alonso and J. A. Dumesic, *Green Chem.*, 2014, **16**, 4816–4838.
6 F. H. Isikgor and C. R. Becer, *Polym. Chem.*, 2015, **6**, 4497–4559.
7 I. Delidovich, P. J. C. Hausoul, L. Deng, R. Pfützenreuter, M. Rose and R. Palkovits, *Chem. Rev.*, 2016, **116**, 1540–1599.
8 G. Guerriero, J. F. Hausman, J. Strauss, H. Ertan and K. S. Siddiqui, *Eng. Life Sci.*, 2016, **16**, 1–16.
9 W. Boerjan, J. Ralph and M. Baucher, *Annu. Rev. Plant Biol.*, 2003, **54**, 519–546.
10 J. Ralph, K. Lundquist, G. Brunow, F. Lu, H. Kim, P. F. Schatz, J. M. Marita, R. D. Hatfield, S. A. Ralph, J. H. Christensen and W. Boerjan, *Phytochem. Rev.*, 2004, **3**, 29–60.
11 R. Vanholme, B. Demedts, K. Morreel, J. Ralph and W. Boerjan, *Plant Physiol.*, 2010, **153**, 895–905.
12 R. Vanholme, B. De Meester, J. Ralph and W. Boerjan, *Curr. Opin. Biotechnol*, 2019, **56**, 230–239.
13 W. Schutyser, T. Renders, S. Van Den Bosch, S. F. Koelewijn, G. T. Beckham and B. F. Sels, *Chem. Soc. Rev.*, 2018, **47**, 852–908.
14 M. V. Galkin and J. S. M. Samec, *ChemSusChem*, 2016, **9**, 1544–1558.
15 J. Zakzeski, P. C. A. Bruijnincx, A. L. Jongerius and B. M. Weckhuysen, *Chem. Rev.*, 2010, **110**, 3552–3599.
16 L. Cao, I. K. M. Yu, Y. Liu, X. Ruan, D. C. W. Tsang, A. J. Hunt, Y. S. Ok, H. Song and S. Zhang, *Bioresour. Technol.*, 2018, **269**, 465–475.
17 S. Van Den Bosch, W. Schutyser, R. Vanholme, T. Driessen, S. F. Koelewijn, T. Renders, B. De Meester, W. J. J. Huijgen, W. Dehaen, C. M. Courtin, B. Lagrain, W. Boerjan and B. F. Sels, *Energy Environ. Sci.*, 2015, **8**, 1748–1763.
18 T. Parsell, S. Yohe, J. Degenstein, T. Jarrell, I. Klein, E. Gencer, B. Hewetson, M. Hurt, J. I. Kim, H. Choudhari, B. Saha, R. Meilan, N. Mosier, F. Ribeiro, W. N. Delgass, C. Chapple, H. I. Kenttämaa, R. Agrawal and M. M. Abu-Omar, *Green Chem.*, 2015, **17**, 1492–1499.
19 P. Ferrini and R. Rinaldi, *Angew. Chem., Int. Ed.*, 2014, **53**, 8634–8639.
20 S. Rautiainen, D. Di Francesco, S. N. Katea, G. Westin, D. N. Tungasmita and J. S. M. Samec, *ChemSusChem*, 2019, **12**, 404–408.
21 E. M. Anderson, R. Katahira, M. Reed, M. G. Resch, E. M. Karp, G. T. Beckham and Y. Román-Leshkov, *ACS Sustainable Chem. Eng.*, 2016, **4**, 6940–6950.
22 X. Huang, J. Zhu, T. I. Korányi, M. D. Boot and E. J. M. Hensen, *ChemSusChem*, 2016, **9**, 3262–3267.
23 L. Shuai, M. T. Amiri, Y. M. Questell-Santiago, F. Héroguel, Y. Li, H. Kim, R. Meilan, C. Chapple, J. Ralph and J. S. Luterbacher, *Science*, 2016, **354**, 329–333.
24 A. De Santi, M. V. Galkin, C. W. Lahive, P. J. Deuss and K. Barta, *ChemSusChem*, 2020, **13**, 4468–4477.
25 S. Bertella, M. B. Figueirêdo, G. De Angelis, M. Mourez, C. Bourmeaud, E. Amstad and J. Luterbacher, *ChemSusChem*, 2022, 1–10.
26 M. M. Abu-Omar, K. Barta, G. T. Beckham, J. S. Luterbacher, J. Ralph, R. Rinaldi, Y. Román-Leshkov, J. S. M. Samec, B. F. Sels and F. Wang, *Energy Environ. Sci.*, 2021, **14**, 262–292.
27 T. Renders, S. Van Den Bosch, S.-F. Koelewijn, W. Schutyser and B. F. Sels, *Energy Environ. Sci.*, 2017, **10**, 1551–1557.
28 T. Renders, G. Van den Bossche, T. Vangeel, K. Van Aelst and B. Sels, *Curr. Opin. Biotechnol*, 2019, **56**, 193–201.
29 S. Van den Bosch, T. Renders, S. Kennis, S.-F. F. Koelewijn, G. den Bossche, T. Vangeel, A. Deneyer, D. Depuydt, C. M. Courtin, J. M. Thevelein, W. Schutyser and B. F. Sels, *Green Chem.*, 2017, **19**, 3313–3326.
30 E. M. Anderson, M. L. Stone, M. J. Hülsey, G. T. Beckham and Y. Román-Leshkov, *ACS Sustainable Chem. Eng.*, 2018, **6**, 7951–7959.

Open Access Article. Published on 02 May 2023. Downloaded on 2/3/2026 7:13:05 AM. This article is licensed under a Creative Commons Attribution 3.0 Unported Licence.

31 E. M. Anderson, M. L. Stone, R. Katahira, M. Reed, W. Muchero, K. J. Ramirez, G. T. Beckham and Y. Román-Leshkov, *Nat. Commun.*, 2019, **10**, 1–10.
32 W. Schutyser, S. Van Den Bosch, T. Renders, T. De Boe, S.-F. F. Koelewijn, A. Dewaele, T. Ennaert, O. Verkinderen, B. Goderis, C. M. Courtin and B. F. Sels, *Green Chem.*, 2015, **17**, 5035–5045.
33 T. Renders, S. Van Den Bosch, T. Vangeel, T. Ennaert, S. F. Koelewijn, G. Van Den Bossche, C. M. Courtin, W. Schutyser and B. F. Sels, *ACS Sustainable Chem. Eng.*, 2016, **4**, 6894–6904.
34 T. Renders, E. Cooreman, S. Van Den Bosch, W. Schutyser, S. F. Koelewijn, T. Vangeel, A. Deneyer, G. Van Den Bossche, C. M. Courtin and B. F. Sels, *Green Chem.*, 2018, **20**, 4607–4619.
35 P. Ferrini, C. A. Rezende and R. Rinaldi, *ChemSusChem*, 2016, **9**, 3171–3180.
36 X. Ouyang, X. Huang, J. Zhu, M. D. Boot and E. J. M. Hensen, *ACS Sustainable Chem. Eng.*, 2019, **7**, 13764–13773.
37 Q. Song, F. Wang, J. Cai, Y. Wang, J. Zhang, W. Yu and J. Xu, *Energy Environ. Sci.*, 2013, **6**, 994–1007.
38 S. Van Den Bosch, W. Schutyser, S.-F. F. Koelewijn, T. Renders, C. M. Courtin and B. F. Sels, *Chem. Commun.*, 2015, **51**, 13158–13161.
39 T. Renders, W. Schutyser, S. Van Den Bosch, S. F. Koelewijn, T. Vangeel, C. M. Courtin, B. F. Sels, S. Van Den Bosch, S. F. Koelewijn and T. Vangeel, *ACS Catal.*, 2016, **6**, 2055–2066.
40 X. Huang, O. M. Morales Gonzalez, J. Zhu, T. I. Korányi, M. D. Boot and E. J. M. Hensen, *Green Chem.*, 2017, **19**, 175–187.
41 M. V. Galkin, A. T. Smit, E. Subbotina, K. A. Artemenko, J. Bergquist, W. J. J. Huijgen and J. S. M. Samec, *ChemSusChem*, 2016, **9**, 3280–3287.
42 C. Li, M. Zheng, A. Wang and T. Zhang, *Energy Environ. Sci.*, 2012, **5**, 6383–6390.
43 K. Van Aelst, E. Van Sinay, T. Vangeel, E. Cooreman, G. Van Den Bossche, T. Renders, J. Van Aelst, S. Van den Bosch and B. F. Sels, *Chem. Sci.*, 2020, **11**, 11498–11508.
44 T. Vangeel, T. Renders, K. Van Aelst, E. Cooreman, S. Van Den Bosch, G. Van Den Bossche, S. Koelewijn, C. M. Courtin and B. F. Sels, *Green Chem.*, 2019, **21**, 5841–5851.
45 A. Adler, I. Kumaniaev, A. Karacic, K. R. Baddigam, R. J. Hanes, E. Subbotina, A. W. Bartling, A. J. Huertas-Alonso, A. Moreno, H. Hakansson, A. P. Mathew, G. T. Beckham and S. M. Joseph, *Joule*, 2022, **6**, 1845–1858.
46 E. M. Anderson, M. L. Stone, R. Katahira, M. Reed, G. T. Beckham and Y. Román-Leshkov, *Joule*, 2017, **1**, 613–622.
47 I. Kumaniaev, E. Subbotina, J. Sävmarker, M. Larhed, M. V. Galkin and J. S. M. Samec, *Green Chem.*, 2017, **19**, 5767–5771.
48 J. H. Jang, D. G. Brandner, R. J. Deriling, A. J. Ringsby, J. R. Bussard, L. M. Stanley, R. M. Happs, A. S. Kovvali, J. I. Cutler, T. Renders, J. R. Bielenberg, Y. Román-Leshkov and G. T. Beckham, *Joule*, 2022, **6**, 1–17.
49 F. Brandi, B. Pandalone and M. Al-Naji, *RSC Sustain.*, 2023, DOI: **10.1039/d2su00076h**.
50 A. W. Bartling, M. L. Stone, R. J. Hanes, A. Bhatt, Y. Zhang, M. J. Biddy, R. Davis, J. S. Kruger, N. E. Thornburg, J. S. Luterbacher, R. Rinaldi, J. S. M. Samec, B. F. Sels, Y. Román-Leshkov and G. T. Beckham, *Energy Environ. Sci.*, 2021, **14**, 4147–4168.
51 A. Deneyer, E. Peeters, T. Renders, S. Van den Bosch, N. Van Oeckel, T. Ennaert, T. Szarvas, T. I. Korányi, M. Dusselier and B. F. Sels, *Nat. Energy*, 2018, **3**, 969–977.
52 Y. Huang, Y. Duan, S. Qiu, M. Wang, C. Ju, H. Cao, Y. Fang and T. Tan, *Sustainable Energy Fuels*, 2018, **2**, 637–647.
53 M. L. Stone, M. S. Webber, W. P. Mounfield, D. C. Bell, E. Christensen, A. R. C. Morais, Y. Li, E. M. Anderson, J. S. Heyne, G. T. Beckham and Y. Román-Leshkov, *Joule*, 2022, **6**, 2324–2337.
54 X. Huang, J. M. Ludenho, M. Dirks, X. Ouyang, M. D. Boot and E. J. M. Hensen, *ACS Catal.*, 2018, **8**, 11184–11190.
55 Y. Liao, S.-F. Koelewijn, G. Van den Bossche, J. Van Aelst, S. Van den Bosch, T. Renders, K. Navare, T. Nicolaï, K. Van Aelst, M. Maesen, H. Matsushima, J. M. Thevelein, K. van Acker, B. Lagrain, D. Verboekend and B. F. Sels, *Science*, 2020, **367**, 1385–1390.
56 A. Wang and T. Zhang, *Acc. Chem. Res.*, 2012, **46**, 1377–1386.
57 R. Palkovits, K. Tajvidi, A. M. Ruppert and J. Procelewska, *Chem. Commun.*, 2011, **47**, 576–578.
58 S. F. Koelewijn, S. Van Den Bosch, T. Renders, W. Schutyser, B. Lagrain, M. Smet, J. Thomas, W. Dehaen, P. Van Puyvelde, H. Witters and B. F. Sels, *Green Chem.*, 2017, **19**, 2561–2570.
59 E. Feghali, D. J. Van De Pas, A. J. Parrott and K. M. Torr, *ACS Macro Lett.*, 2020, **9**, 1155–1160.
60 E. Feghali, D. J. Van De Pas and K. M. Torr, *Biomacromolecules*, 2020, **21**, 1548–1559.
61 M. A. Jedrzejczyk, N. Madelat, B. Wouters, H. Smeets, M. Wolters, S. A. Stepanova, T. Vangeel, K. Van Aelst, S. Van den Bosch, J. Van Aelst, V. Polizzi, K. Servaes, K. Vanbroekhoven, B. Lagrain, B. F. Sels, H. Terryn and K. V. Bernaerts, *Macromol. Chem. Phys.*, 2022, **2100461**, 1–10.
62 K. Van Aelst, E. Van Sinay, T. Vangeel, Y. Zhang, T. Renders, S. Van den Bosch, J. Van Aelst and B. F. Sels, *Chem. Commun.*, 2021, **57**, 4–7.
63 M. A. Jedrzejczyk, S. Van den Bosch, J. Van Aelst, K. Van Aelst, P. D. Kouris, M. Moalin, G. R. M. M. Haenen, M. D. Boot, E. J. M. Hensen, B. Lagrain, B. F. Sels and K. V. Bernaerts, *ACS Sustainable Chem. Eng.*, 2021, **9**, 12548–12559.
64 D. Ruijten, T. Narmon, K. Van Aelst, H. De Weer, R. Van der Zweep, T. Hendrickx, C. Poleunis, L. Li, K. M. Van Geem, D. P. Debecker and B. F. Sels, *ACS Sustainable Chem. Eng.*, 2023, **11**, 4776–4788.
65 E. Cooreman, T. Vangeel, K. Van Aelst, J. Van Aelst, J. Lauwaert, J. Thybaut, S. Van den Bosch and B. Sels, *Ind. Eng. Chem. Res.*, 2020, **59**, 17035–17045.
66 Z. Sun, J. Cheng, D. Wang, T. Q. Yuan, G. Song and K. Barta, *ChemSusChem*, 2020, **13**, 5199–5212.

 This journal is © The Royal Society of Chemistry 2023

Open Access Article. Published on 02 May 2023. Downloaded on 2/3/2026 7:13:05 AM.
This article is licensed under a Creative Commons Attribution 3.0 Unported Licence.

67 Z. Sultan, I. Graça, Y. Li, S. Lima, L. G. Peeva, D. Kim, M. A. Ebrahim, R. Rinaldi and A. G. Livingston, *ChemSusChem*, 2019, **12**, 1203–1212.
68 W. Arts, D. Ruijten, K. Van Aelst, L. Trullemans and B. Sels, *Catalysis in Biomass Conversion*, Elsevier Inc., 1st edn, 2021, pp. 1–57.
69 M. Tschulkow, T. Compernolle, S. Van den Bosch, J. Van Aelst, I. Storms, M. Van Dael, G. Van den Bossche, B. Sels and S. Van Passel, *J. Clean. Prod.*, 2020, **266**, 1–11.
70 T. Pöpken, L. Götze and J. Gmehling, *Ind. Eng. Chem. Res.*, 2000, **39**, 2601–2611.
71 Fuel Cells and Hydrogen Joint Undertaking, Hydrogen Roadmap Europe, **https://www.fch.europa.eu/publications/hydrogen-roadmap-europe-sustainable-pathway-european-energy-transition**, (accessed 5 May 2022).
72 L. R. Lynd, G. T. Beckham, A. M. Guss, L. N. Jayakody, E. M. Karp, C. Maranas, R. L. McCormick, D. Amador-Noguez, Y. J. Bomble, B. H. Davison, C. Foster, M. E. Himmel, E. K. Holwerda, M. S. Laser, C. Y. Ng, D. G. Olson, Y. Román-Leshkov, C. T. Trinh, G. A. Tuskan, V. Upadhayay, D. R. Vardon, L. Wang and C. E. Wyman, *Energy Environ. Sci.*, 2022, **15**, 938–990.
73 S. F. Koelewijn, C. Cooreman, T. Renders, C. Andecochea Saiz, S. Van Den Bosch, W. Schutyser, W. De Leger, M. Smet, P. Van Puyvelde, H. Witters, B. Van Der Bruggen and B. F. Sels, *Green Chem.*, 2018, **20**, 1050–1058.
74 K. Navare, W. Arts, G. Faraca, G. Van Den Bossche, B. Sels and K. Van, *Resour., Conserv. Recycl.*, 2022, **186**, 106588.
75 G. Guest, F. Cherubini and A. H. Strømman, *J. Ind. Ecol.*, 2013, **17**, 20–30.
76 I. Kumaniaev and J. S. M. Samec, *Ind. Eng. Chem. Res.*, 2019, **58**, 6899–6906.
77 H. Dao Thi, K. Van Aelst, S. Van den Bosch, R. Katahira, G. T. Beckham, B. F. Sels and K. M. Van Geem, *Green Chem.*, 2022, **24**, 191–206.
78 S. Steven, European pulp prices: BEK moved up again while NBSK spread widened in July, **https://www.fastmarkets.com/insights/european-pulp-prices-continue-to-rise-in-july-2022**.
79 N. E. Thornburg, M. B. Pecha, D. G. Brandner, M. L. Reed, J. V. Vermaas, W. E. Michener, R. Katahira, T. B. Vinzant, T. D. Foust, B. S. Donohoe, Y. Román-Leshkov, P. N. Ciesielski and G. T. Beckham, *ChemSusChem*, 2020, **13**, 4495–4509.
80 R. Rowell, R. Pettersen and M. Tshabalala, in *Handbook of Wood Chemistry and Wood Composites*, ed. R. M. Rowell, C. R. C. Press, 2nd edn, 2012, pp. 33–72.
81 R. Sinnott and G. Towler, *Chemical Engineering Design*, Elsevier, 5th edn, 2009, pp. 291–388.
82 E. Nieuwlaar, A. L. Roes and M. K. Patel, *J. Ind. Ecol.*, 2015, **20**, 828–836.
83 P. Breeze, *Gas-Turbine Power Generation*, Elsevier, 2016, pp. 93–98.
84 H. N. Englyst and J. H. Cummings, *Analyst*, 1984, **109**, 937–942.
85 C. Gourson, R. Benhaddou, R. Granet, P. Krausz, B. Verneuil, P. Branland, G. Chauvelon, J. F. Thibault and L. Saulnier, *J. Appl. Polym. Sci.*, 1999, **74**, 3040–3045.
86 J. Snelders, E. Dornez, B. Benjelloun-Mlayah, W. J. J. Huijgen, P. J. de Wild, R. J. A. Gosselink, J. Gerritsma and C. M. Courtin, *Bioresour. Technol.*, 2014, **156**, 275–282.
87 A. Sluiter, B. Hames, R. Ruiz, C. Scarlata, J. Sluiter, D. Templeton and D. Crocker, *Determination of structural carbohydrates and lignin in biomass*, 2012.
88 M. Condon, *ICIS Chem. Bus.*, 2019, **1–7**, 19.
89 F. J. London, *ICIS Chem. Bus.*, 2020, **14–20**, 32.
90 Anonymous, *ICIS Chem. Bus.*, 2020, **9–15**, 15.